GGCC-3′) and its mismatch scrambled oligodeoxynucleotide (MS-ODN; 5′-GTCGTCGGCGGAGCA-3′) were synthesized and freshly dissolved in artificial CSF (aCSF) containing the following (in mM): 125 NaCl, 3.8 KCl, 2.0 $CaCl_2$, 1.0 $MgCl_2$, 1.2 KH_2PO_4, 26 $NaHCO_3$, 10 glucose, pH 7.4). AS-ODN or MS-ODN was intrathecally injected at a dose of 10 μg per 5 μl of aCSF on the first, third, and fifth days. Then, nerve injury was performed with subsequent injections of AS-ODN on days 1, 3, 5, and 6 postinjury. The mRNA levels, pain thresholds, peripheral morphine analgesia, and peripheral A-803467 hypoesthesia were assessed at day 7 postinjury.

Nociception test. In thermal paw withdrawal tests, the nociception threshold was evaluated by the latency of paw withdrawal upon a thermal stimulus (Hargreaves et al., 1988; Inoue et al., 2004). Unanesthetized animals were placed in Plexiglas cages on top of a glass sheet, and an adaptation period of 1 h was allowed. The thermal stimulator (IITC Life Science) was positioned under the glass sheet and the focus of the projection bulb was aimed exactly at the middle of the plantar surface of the animal. A mirror attached to the stimulator permitted visualization of the plantar surface. A cutoff time of 20 s was set to prevent tissue damage. The mechanical paw pressure test was performed as described previously (Rashid et al., 2003; Inoue et al., 2004). Briefly, mice were placed in a Plexiglas chamber on a 6 × 6 mm wire mesh grid floor and allowed to acclimatize for a period of 1 h. A mechanical stimulus was then delivered to the middle of the plantar surface of the right hindpaw using a transducer indicator (model 1601; IITC Life Science). The pressure needed to induce a flexor response was defined as the pain threshold. A cutoff pressure of 20 g was set to avoid tissue damage. In these experiments, using mechanical and thermal tests, the thresholds were determined from three repeated challenges at 10 min intervals, and the averages of responses were evaluated. An electrical stimulation-induced paw withdrawal (EPW) test was performed as described previously (Matsumoto et al., 2008). Briefly, electrodes (Neurotron) were fastened to the plantar surfaces and insteps of mice. Transcutaneous nerve stimuli with each of the three sine-wave pulses (5, 250, and 2000 Hz) were applied using a Neurometer CPT/C system (Neurotron). The minimum intensity (μA) at which each mouse withdrew its paw was defined as the current stimulus threshold. Investigators blind to drug treatments performed all behavioral experiments.

Drug treatments. Morphine hydrochloride (Takeda Chemical Industries) was dissolved in physiological saline. Saline was used for control injections. Intraplantar injections were given using a Hamilton microsyringe connected to polyethylene tubing with a 30 gauge hypodermic needle. For the time course experiment, we measured the paw-withdrawal latencies at every 10 min interval until 60 min after intraplantar injection of morphine (30 nmol), as reported previously (Rashid et al., 2004). In the area under the curve analysis of peripheral morphine analgesia, we calculated the area under the curve generated by plotting analgesic threshold (after deducting the control threshold from each threshold point) against time, from 10 to 60 min after morphine treatment, using a trapezoidal method. A-803467 (Biomol), a selective blocker for $Na_v1.8$ (Jarvis et al., 2007), was dissolved in dimethyl sulfoxide. Before administration, A-803467 was diluted 15-fold for intraperitoneal injection and 28-fold for intraplantar injection in saline, respectively. The EPW test was performed 30 min after intraperitoneal injection of A-803467 (10 mg/kg), as reported previously (Jarvis et al., 2007).

Quantitative real-time PCR. Total RNA was extracted from L4-6 DRGs using TRIzol (Invitrogen), and 500 ng of RNA was used for cDNA synthesis. Quantitative real-time PCR was performed with qPCR MasterMix Plus for SYBR Green I (Eurogentec) using the ABI Prism 7000 sequence detection system (Applied Biosystems). The PCR primers used are listed in supplemental Table 1, available at www.jneurosci.org as supplemental material. Some of the primers were published previously (Koenigsberger et al., 2000; Klein et al., 2003; Qiang et al., 2005; Matsumoto et al., 2006; Cheng et al., 2009; Staaf et al., 2009). Glyceraldehyde-3-phosphate dehydrogenase (GAPDH) was used as an internal control for normalization. In all cases, the validity of amplification was confirmed by the presence of a single peak in the melting temperature analysis and by linear amplification with increasing number of PCR cycles.

Western blot analysis. The L4-6 DRGs from three mice were pooled. DRG samples were homogenized twice in ice-cold cell lysis buffer [10 mM Tris-HCl, pH 8.0, 10 mM NaCl, 0.2% Nonidet P-40, 1 μM (p-amidinophenyl)methanesulfonyl fluoride hydrochloride (p-APMSF)], and then the homogenates were centrifuged to remove contaminating cytosol. Crude nuclear fractions (30 μg) were separated by SDS-PAGE on 7.5% (NRSF) or 15% (histone H3) gels. The primary antibodies were used in the following dilutions: NRSF (1:500; Millipore) and histone H3 (1:500; Millipore). Immunoreactive signals for NRSF (200 kDa) and histone H3 (17 kDa) were detected using enhanced chemiluminescent substrate (SuperSignal West Pico chemiluminescent substrate; Pierce).

Immunohistochemistry. Mice were deeply anesthetized with pentobarbital (50 mg/kg, i.p.) and perfused transcardially with 20 ml of potassium-free PBS (K^+-free PBS, pH 7.4), followed by 50 ml of a 4% paraformaldehyde solution. The L4-6 DRGs were isolated, postfixed for 3 h, and cryoprotected overnight in a 25% sucrose solution. Tissues were fast frozen in cryo-embedding compound in a mixture of ethanol and dry ice and stored at −80°C until use. DRGs were cut on a cryostat at a thickness of 10 μm, thaw mounted on silane-coated glass slides, and air dried overnight at room temperature (RT). Before immunolabeling, antigen unmasking was performed by microwave treatment three times (10 min each) in 10 mM citrate buffer (pH 6.0). The DRG sections were then incubated with 50 and 100% methanol for 5 min, respectively, and washed with PBST (0.1% Triton X-100 in K^+-free PBS). The sections were incubated with blocking buffer containing 3% BSA in PBST and subsequently reacted with rabbit polyclonal NRSF antibody (1:200) overnight at 4°C. After washing, the sections were incubated with secondary antibody, Alexa Fluor 594-conjugated anti-rabbit IgG (1:300; Invitrogen), for 2 h at RT. For double immunolabeling, we used the following antibodies: mouse monoclonal antibody against neuron-specific nuclear protein (anti-NeuN; 1:500; Millipore) and Alexa Fluor 488-conjugated anti-mouse IgG (1:300; Invitrogen). After washing, the sections were mounted with Shandon PermaFluor (Thermo Scientific) and analyzed using a confocal laser scanning microscope (PASCAL, Zeiss).

Chromatin immunoprecipitation assay. Chromatin immunoprecipitation (ChIP) assays were performed using protocols from Millipore and from a previous report (Kubat et al., 2004) with some modifications. For each ChIP assay, the L4-6 DRGs from two mice were pooled. DRG samples were homogenized in ice-cold cell lysis buffer (10 mM Tris-HCl, pH 8.0, 10 mM NaCl, 0.2% Nonidet P-40, 1 μM p-APMSF). Samples were then cross-linked in PBS containing 1% formaldehyde at 37°C for 5 min. The cross-linking reaction was terminated with glycine (0.125 M) and, after repeated washing with PBS, the samples were resuspended in SDS lysis buffer (50 mM Tris-HCl, pH 8.1, 10 mM EDTA, 1% SDS, 1 μM p-APMSF). The chromatin was sheared by sonication into 200–500 bp fragments. Ten percent of each lysate was used as the input control for normalization. The sheared chromatin was diluted 10-fold in ChIP dilution buffer (16.7 mM Tris-HCl, pH 8.1, 1.2 mM EDTA, 167 mM NaCl, 1.1% Triton X-100, 0.01% SDS, 1 μM p-APMSF) and then precleared with protein A-agarose beads (Millipore) for 45 min at 4°C with rotation. The supernatant was incubated overnight at 4°C with anti-NRSF (5 μg), anti-acetyl-H3 (5 μg; Millipore), anti-acetyl-H4 antibodies (5 μl; Millipore), or normal rabbit IgG (5 μg; Santa Cruz Biotechnology). Complexes were collected for 2 h using protein A-agarose beads. Following washing and elution steps, cross-linking was reversed at 65°C for 4 h in the presence of 0.2 M NaCl. After proteinase K treatment for 1 h at 45°C, DNA was purified by phenol/chloroform extraction, dissolved in 50 μl of TE buffer (10 mM Tris-HCl, pH 8.0, 1 mM EDTA), and used for PCR. The PCR products were analyzed on a 2% agarose gel. PCR primers used are listed in supplemental Table 1, available at www.jneurosci.org as supplemental material. The primers for MOP-NRSE were published previously (Kim et al., 2004). Quantitative real-time PCR was performed as described above. In all cases, the validity of amplification was confirmed by the presence of a single peak in the melting temperature analysis and by linear amplification with increasing number of PCR cycles.

Statistical analysis. The differences between multiple groups were analyzed using a one-way ANOVA with Tukey–Kramer multiple-comparison *post hoc* analysis (see Figs. 4*B*, *C*, 5, 6*B*; also see supplemental Fig. S2, available at www.jneurosci.org as supplemental material). Data were analyzed using Student's *t* test (see Figs. 1*A*, 2, 3, 4*A*, 6*A*; also see

supplemental Fig. S3, available at www.jneurosci.org as supplemental material). The criterion of significance was set at $p < 0.05$. All results are expressed as means ± SEM.

Results

Downregulations of NRSE-containing MOP and $Na_v1.8$ gene expressions

To validate that MOP and $Na_v1.8$ are downregulated at the transcriptional level, we isolated L4-6 DRGs at days 1, 3, 7, and 14 postinjury, and mRNA expression levels were quantified by real-time PCR. We found that nerve injury causes a long-lasting reduction in MOP and $Na_v1.8$ mRNA levels in the DRG, starting from days 1 and 3 postinjury, respectively, and these downregulations persisted at least 14 d postinjury (Fig. 1*A*).

As reported previously (Kim et al., 2004), analysis using the TFSEARCH program (version 1.3, http://www.cbrc.jp/research/db/TFSEARCHJ.html) with a threshold score of 80.0 revealed that the MOP gene contains a 21 bp NRSE sequence at initiation codon (Fig. 1*B*), which is highly conserved among mouse, rat, and human (Fig. 1*C*). Based on a previous report indicating the presence of a NRSE in the $Na_v1.8$ gene (Otto et al., 2007), we analyzed its location and sequence. We found that the mouse $Na_v1.8$ gene contains two putative conserved NRSE sites, a forward-oriented sequence within the 5′-untranslated region (NRSE-1) and a reverse-oriented sequence within intron 10 (NRSE-2) (Fig. 1*B*,*C*). Rat and human $Na_v1.8$ genes contain unique NRSEs within the intron 3′ and 5′-untranslated region, respectively (Fig. 1*B*,*C*). Within all NRSE sequences of these genes, the GG nucleotides known to be important for NRSF binding (Mori et al., 1992) were completely conserved (Fig. 1*C*).

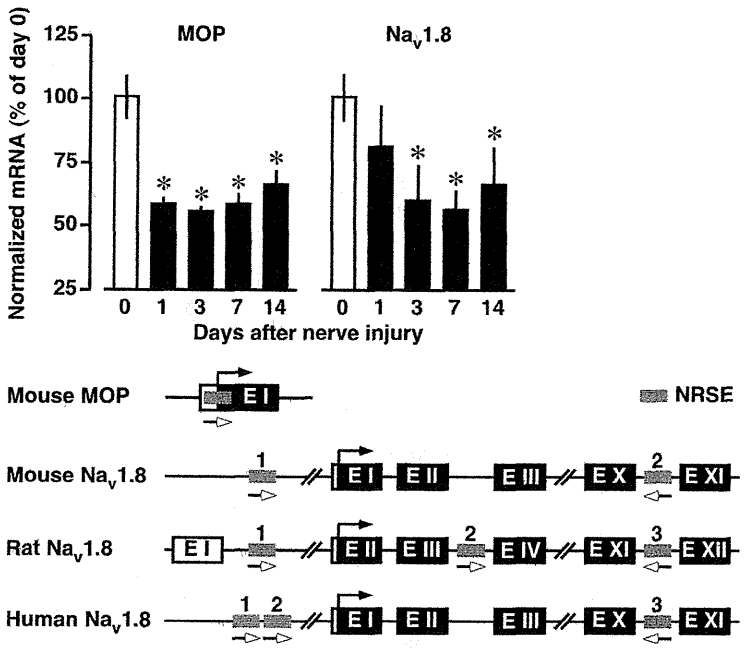

C

Gene	Sequence	Position (score)
Consensus NRSE	ttCAGCACCacGGACAGcgcC	
Mouse MOP NRSE	-----A----t-------ag-	-9/+12 (87.5)
Rat MOP NRSE	----------t-------ag-	-9/+12 (93.0)
Human MOP NRSE	g----T----t-------ag-	-9/+12 (84.1)
Mouse $Na_v1.8$ NRSE-1	----------------a--A	-12593/-12573 (95.0)
Mouse $Na_v1.8$ NRSE-2	----------g------a--T	+30025/+30005 (90.9)
Rat $Na_v1.8$ NRSE-1	a----------------a---	-13896/-13876 (94.8)
Rat $Na_v1.8$ NRSE-2	c------T--a--G----c--	+3998/+4018 (80.3)
Rat $Na_v1.8$ NRSE-3	----------g------a--T	+30131/+30111 (90.9)
Human $Na_v1.8$ NRSE-1	-----T-------T----t-A	-12005/-11985 (84.3)
Human $Na_v1.8$ NRSE-2	-----A----t---T-----A	-11957/-11937 (82.1)
Human $Na_v1.8$ NRSE-3	c----------------g-aA	+38697/+38677 (86.3)

Figure 1. Downregulation of NRSE-containing MOP and $Na_v1.8$ genes after nerve injury. ***A***, Time course of MOP and $Na_v1.8$ mRNA expressions in the DRG after nerve injury. The mRNA expression levels were assessed using quantitative real-time PCR and normalized to that of GAPDH mRNA. Data are calculated as percentages of day 0 and expressed as the means ± SEM from at least three mice, $*p < 0.05$ versus day 0. ***B***, Schematic diagram indicating the locations of NRSE sequences within MOP and $Na_v1.8$ genes. Coding exons are shown as black boxes, the noncoding exons as open boxes, and the NRSE sequences as gray boxes. The black arrows indicate the translation initiation sites, and the lower open arrows indicate the orientation of the NRSE sequences. ***C***, Deviations of MOP- and $Na_v1.8$-NRSEs from the consensus NRSE. The capital letters are conserved among functional NRSE sequences, and the bold capital letters are important for NRSF binding. The scores were obtained from the TFSEARCH program.

Epigenetic upregulation of NRSF expression after nerve injury

The expression level of NRSF regulates its silencing activity (Chong et al., 1995; Schoenherr and Anderson, 1995); therefore, we examined NRSF expression in the DRG after nerve injury. As shown in Figure 2*A*, NRSF mRNA levels were induced 1–14 d postinjury, which is negatively correlated with the temporal expression patterns of MOP and $Na_v1.8$ (Fig. 1*A*). When the transcription of three 5′ noncoding exons (I, II, or III) upstream of a common 3′ coding exon IV (Koenigsberger et al., 2000) was separately quantified, it was revealed that all NRSF transcripts, except those containing exon III, were upregulated at day 7 postinjury (Fig. 2*B*). The most prominent induction was observed in the exon II-containing transcript (Fig. 2*B*). Then, we assessed the acetylation of histones H3 and H4, which is correlated with transcriptional activation at the NRSF promoter II, upstream of exon II. ChIP analysis revealed that nerve injury causes a robust increase in the acetylation of histone H4, but not of H3, in the NRSF promoter II region (Fig. 2*C*), which includes putative transcription start sites and binding sites for AP-1 and Sp1. Furthermore, to assess whether the altered transcription might be reflected in its protein abundance, we performed Western blot analysis using anti-NRSF antibody. We found a significant increase in NRSF protein expression at day 7 postinjury (Fig. 2*D*). Using immunohistochemical analysis, we found that almost all NRSF-positive signals are colocalized with NeuN-positive signals in the DRG of sham-operated mice (Fig. 2*E*), suggesting that NRSF is extensively expressed in the DRG neurons. Moreover, nerve injury markedly increased NRSF-positive signals in NeuN-positive DRG neurons at day 7 after injury (Fig. 2*E*).

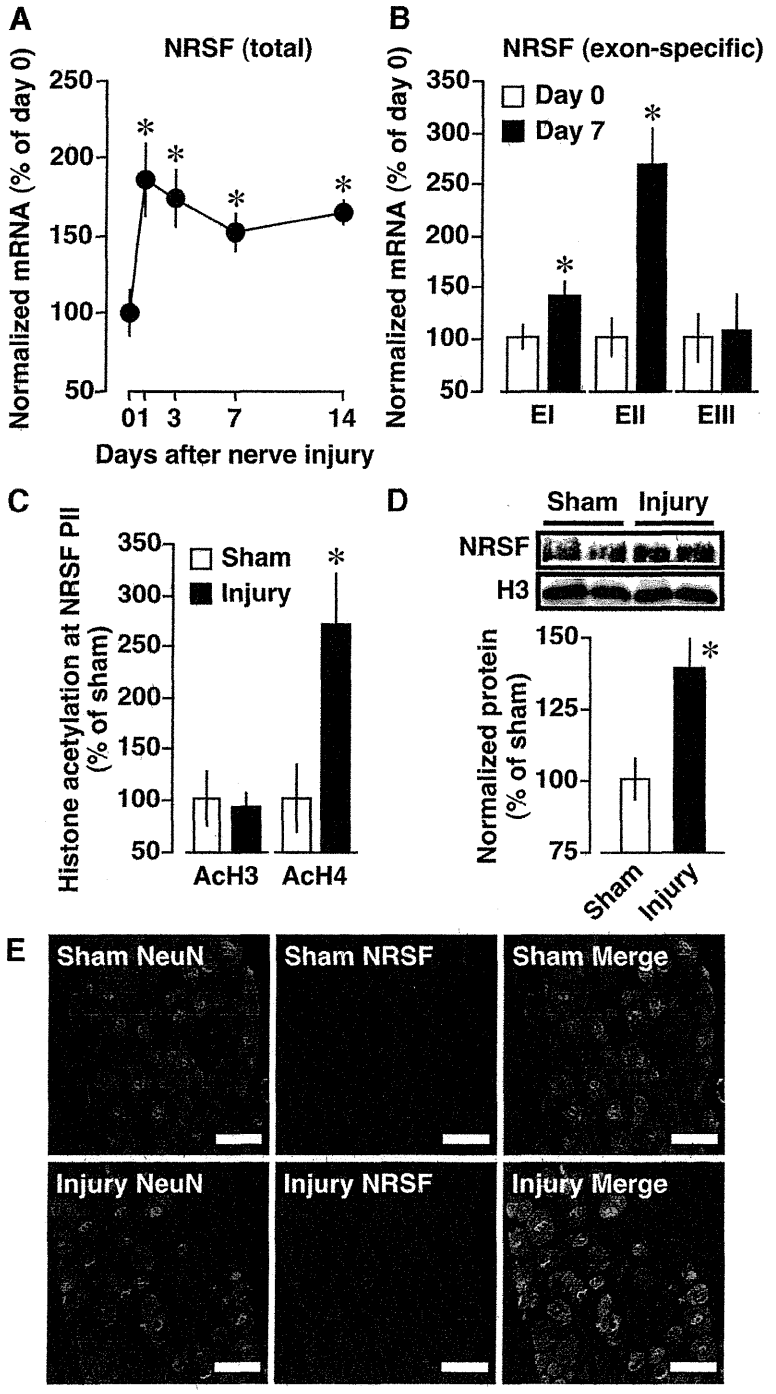

Figure 2. Epigenetic upregulation of NRSF gene expression. ***A***, ***B***, Time course of total (***A***) and exon-specific (***B***) NRSF mRNA expressions in the DRG after nerve injury. The mRNA expression levels were assessed using quantitative real-time PCR and normalized to that of GAPDH mRNA. Data are calculated as percentages of day 0. $*p < 0.05$ versus day 0. EI, EII, EIII, Exons I, II, III, respectively. ***C***, Acetylation of histone H3 (AcH3) and H4 (AcH4) at NRSF promoter II (PII) at day 7 after injury, assessed using ChIP assay. Quantitative analysis was performed using real-time PCR, and the data were normalized to the corresponding input. ***D***, NRSF protein expression at day 7 postinjury, assessed using Western blot analysis. Results are normalized to the histone H3 protein expression level. For ***C*** and ***D***, data are calculated as percentages of sham-operated group. $*p < 0.05$ versus sham-operated group. Data are expressed as the means ± SEM from at least three mice. ***E***, Immunohistochemical double labeling between NRSF (red) and NeuN (green), a neuronal marker, in the DRG of sham-operated and nerve-injured mice. Scale bars, 50 μm.

Histone hypoacetylation with an increase in NRSF binding at NRSE sequences within MOP and $Na_v1.8$ genes

Next, we used ChIP analysis to examine whether NRSF binds to the NRSE sites of MOP and $Na_v1.8$ genes after nerve injury. Nerve injury caused a drastic increase in NRSF binding to MOP-NRSE, $Na_v1.8$-NRSE-1, and $Na_v1.8$-NRSE-2 sequences (Fig. 3*A*), suggesting that these NRSE sequences are capable of serving as NRSF-binding sites. Quantitative real-time PCR analysis showed that there was a threefold increase in NRSF binding to MOP-NRSE and $Na_v1.8$-NRSE-2 (Fig. 3*B*), while the fold change could not be calculated in the NRSF binding to $Na_v1.8$-NRSE-1 because no significant signal was detected in sham-operated preparations (supplemental Fig. S1, available at www.jneurosci.org as supplemental material). In contrast, negligible binding was observed following precipitation by normal IgG, confirming the specificity of the immunoprecipitation (Fig. 3*A*; supplemental Fig. S1, available at www.jneurosci.org as supplemental material). In addition, we performed scanning ChIP analysis to assess the levels of histone H3 and H4 acetylation in the genomic regions spanning NRSE sequences of MOP and $Na_v1.8$ genes. We found significant reductions of histone H3 and H4 acetylation at MOP-NRSE and $Na_v1.8$-NRSE-2 and H3 acetylation at $Na_v1.8$-NRSE-1 at day 7 after injury (Fig. 3*C*,*D*). Together, these data suggest that nerve injury induces repressive chromatin states around the NRSE sequences of MOP and $Na_v1.8$ genes through NRSF-HDAC-mediated mechanisms.

Blockade of nerve injury-induced reductions in MOP and $Na_v1.8$ gene expressions by NRSF knockdown

To examine whether NRSF could contribute to the downregulation of MOP and $Na_v1.8$ genes after nerve injury, mice were intrathecally pretreated with an AS-ODN against NRSF or a corresponding MS-ODN. Western blot analysis revealed that NRSF protein levels in the DRG were markedly reduced by AS-ODN, but not by MS-ODN (Fig. 4*A*). AS-ODN significantly blocked the nerve injury-induced downregulation of MOP and $Na_v1.8$ (Fig. 4*B*). However, AS-ODN had no effects on basal MOP and $Na_v1.8$ mRNA levels in sham-operated mice (Fig. 4*B*). These findings strongly suggest that NRSF-mediated mechanisms are responsible for the transcriptional suppression of MOP and $Na_v1.8$ genes in the DRG after nerve injury.

On the other hand, it has been reported that nerve injury downregulates transient receptor potential melastatin 8 (TRPM8), TRP ankyrin 1 (TRPA1), and calcitonin gene-related peptide (CGRP) in the DRG (Hökfelt et al., 2006; Caspani et al., 2009; Staaf et al., 2009). Using TFSEARCH program, we found that these genes have putative NRSE sites, which

give the TFSEARCH scores below our threshold value, 80.0. However, AS-ODN treatments blocked TRPM8 and TRPA1, but not CGRP, downregulations in the DRG after nerve injury (Fig. 4C).

Recovery of C-fiber function by NRSF knockdown

We next examined abnormal pain behaviors in AS-ODN-treated mice, including C-fiber hypoesthesia, A-fiber hypersensitization, thermal hyperalgesia, and mechanical allodynia. Using the EPW test to evaluate C-, Aδ-, and Aβ-fiber functions after nerve injury (Koga et al., 2005; Matsumoto et al., 2008; Ueda, 2008), we found that AS-ODN significantly blocks hypoesthesia, seen in response to 5 Hz (C-fiber) stimuli, but does not block hypersensitization, seen in response to 250 Hz (Aδ-fiber) or 2000 Hz (Aβ-fiber) stimuli (Fig. 5A–C). However, thermal hyperalgesia and mechanical allodynia after nerve injury were normally manifested in AS-ODN-treated mice (supplemental Fig. S2, available at www.jneurosci.org as supplemental material). On the other hand, AS-ODN had no effects on the basal threshold to thermal, mechanical, and electrical stimuli in sham-operated mice (Fig. 5A–C; supplemental Fig. S2, available at www.jneurosci.org as supplemental material). Consistent with the data for AS-ODN, the treatment with A-803467 (10 mg/kg, i.p.), a selective blocker for $Na_v1.8$ (Jarvis et al., 2007), resulted in a hypoesthesia of C-fiber (control, 93.3 ± 1.7 μA; A-803467, 122.5 ± 7.5 μA; $p < 0.05$ using Student's t test, $n = 3$), but not Aδ-fiber (control, 220.0 ± 20.8 μA; A-803467, 210.0 ± 11.5 μA; $n = 3$) and Aβ-fiber (control, 390.0 ± 10.0 μA; A-803467, 413.3 ± 6.7 μA; $n = 3$). Moreover, 30 nmol, but not 10 nmol, of intraplantar injection of A-803467 produced C-fiber hypoesthesia in naive mice, and the maximal response was observed at 30 min after injection (supplemental Fig. S3, available at www.jneurosci.org as supplemental material). We found that A-803467 (30 nmol, i.pl.)-induced C-fiber hypoesthesia was diminished after nerve injury, and this loss was significantly recovered by AS-ODN (Fig. 5D).

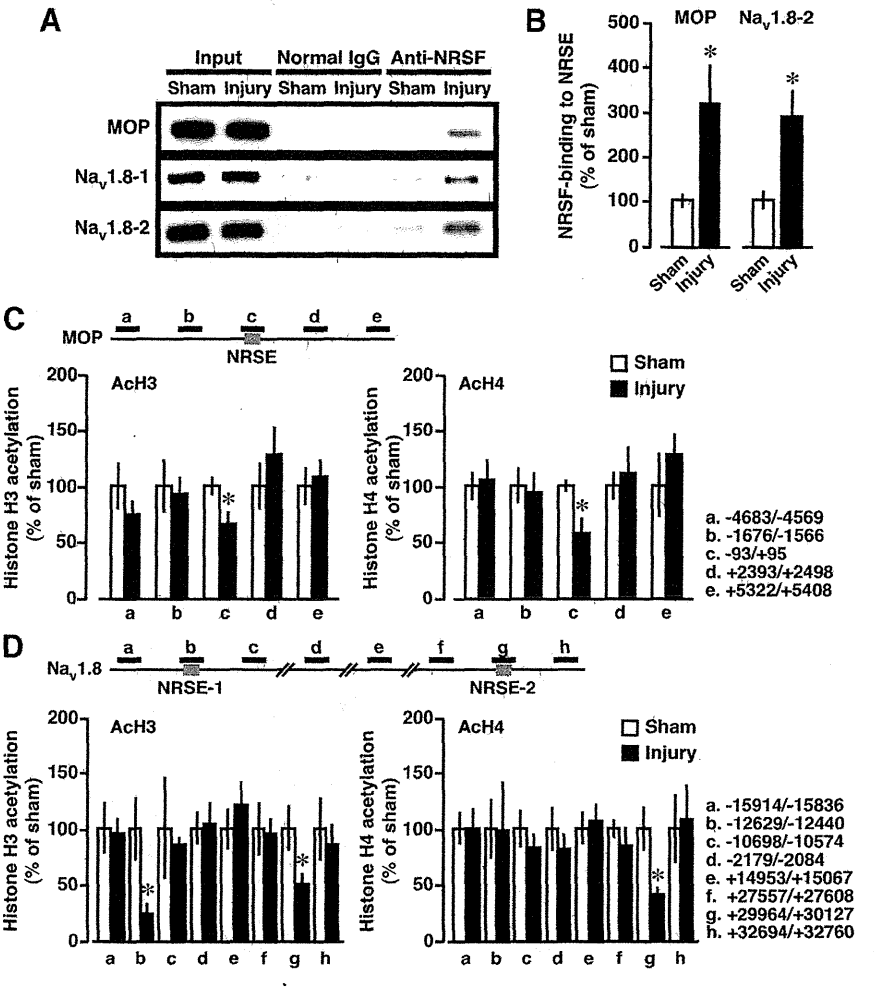

Figure 3. Epigenetic silencing of MOP and $Na_v1.8$ genes through NRSF binding. ChIP assay was performed at day 7 postinjury. *A*, *B*, ChIP assays using anti-NRSF antibody. *A*, Gel images show the representative data. *B*, Quantification of NRSF-binding at MOP-NRSE and at $Na_v1.8$-NRSE-2 ($Na_v1.8$–2). *C*, *D*, Scanning ChIP analysis of acetylation levels of histone H3 (AcH3) and H4 (AcH4) in the genomic regions spanning NRSE sequences within MOP (*C*) and $Na_v1.8$ (*D*) genes. The schematics at the top show the PCR-targeted regions. Quantitative analysis was performed using real-time PCR, and the data were normalized to the corresponding input. Results are calculated as percentages of sham-operated group and expressed as means ± SEM from at least three mice. *$p < 0.05$ versus sham-operated group.

Recovery from nerve injury-induced loss of peripheral morphine analgesia by NRSF knockdown

We examined whether AS-ODN ameliorates the loss of peripheral morphine analgesia, which is due to reduced MOP expression in the DRG neurons after nerve injury (Rashid et al., 2004). In this study, we chose a 30 nmol intraplantar morphine injection, which shows a local analgesic effect in the ipsilateral paw but not in the contralateral paw (Rashid et al., 2004). Consistent with the temporal expression pattern of MOP in the DRG after nerve injury (Fig. 1A), peripheral morphine analgesia was markedly diminished within 3 d after injury (data not shown). The reduced peripheral morphine analgesia at day 7 postinjury was significantly recovered following AS-ODN, but not MS-ODN, administration (Fig. 6A,B). In contrast, peripheral morphine analgesia in sham-operated mice was not altered by AS-ODN (Fig. 6A,B), consistent with the mRNA analysis data (Fig. 4B).

Discussion

Here, we demonstrated the following novel findings: (1) Nerve injury caused an epigenetic induction of NRSF gene expression in the DRG neurons. (2) Nerve injury induces histone hypoacetylation at NRSE sequences within MOP and $Na_v1.8$ genes with an increase in direct NRSF binding. (3) The antisense knockdown of NRSF significantly blocked nerve injury-induced transcriptional repression of MOP, $Na_v1.8$, TRPM8, and TRPA1, but not CGRP, genes in the DRG. (4) All of the nerve injury-induced C-fiber hypoesthesia and the losses of peripheral A-803467 hypoesthesia and peripheral morphine analgesia were markedly recovered by NRSF knockdown.

NRSF is known to repress numerous genes that are essential for neuronal functions, such as ion channels, neurotransmitter receptors, and synaptic vesicle proteins (Schoenherr et al., 1996; Bruce et al., 2004; Otto et al., 2007). It has been reported that

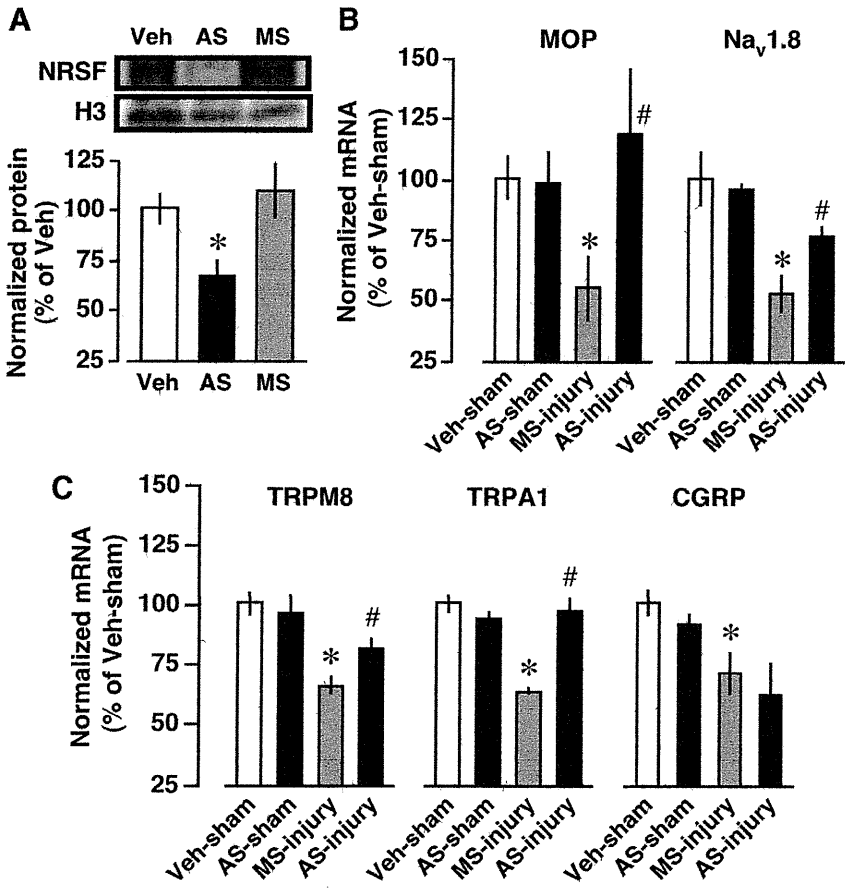

Figure 4. Blockade of nerve injury-induced MOP and $Na_v1.8$ downregulations by NRSF knockdown. Mice were intrathecally pretreated with vehicle (Veh), AS-ODN (AS) against NRSF, or the corresponding MS-ODN (MS). ***A***, AS-ODN-induced reduction of NRSF protein expression in the DRG, assessed by Western blot analysis. Data are normalized to histone H3 protein expression levels and then expressed as percentages of the levels in the Veh-treated group. $*p < 0.05$ versus Veh-treated group. Data represent the means ± SEM from three mice. ***B***, ***C***, The effects of NRSF AS-ODN on nerve injury-induced downregulations of MOP and $Na_v1.8$ (***B***) and TRPM8, TRPA1, and CGRP (***C***) in the DRG at day 7 postinjury. The mRNA expression levels were quantified by real-time PCR, and normalized to that of GAPDH mRNA. Results are calculated as percentages of Veh-treated and sham-operated groups and expressed as means ± SEM from at least three mice, $*p < 0.05$ versus Veh-treated and sham-operated groups and $^{\#}p < 0.05$ versus MS-ODN-treated and nerve-injured groups.

NRSF expression is dramatically decreased to negligible levels during the differentiation of cells into mature neurons, this being concomitant with the upregulation of NRSF target genes (Ballas et al., 2005). However, accumulating evidence has revealed that NRSF expression is detected in the adult brain as well as in DRG (Palm et al., 1998; Mori et al., 2002). The present study demonstrated that peripheral nerve injury upregulates NRSF mRNA and protein expression in the DRG, thereby causing epigenetic silencing of MOP and $Na_v1.8$ genes. Considering that NRSF is upregulated after nerve injury in substantially all DRG neurons, it is likely that NRSF-mediated MOP and $Na_v1.8$ downregulations occur in the neuronal populations of DRG. In contrast to the blockade of nerve injury-induced downregulation of MOP and $Na_v1.8$ by NRSF AS-ODN, NRSF knockdown had no effects on basal expression levels of MOP and $Na_v1.8$ in sham-operated mice. Previous reports have suggested that NRSF acts in a concentration-dependent manner, and its silencing activity is insufficient when its expression is below that of a threshold level (Chong et al., 1995; Schoenherr and Anderson, 1995). The present study strongly indicates the presence of such threshold expression levels of NRSF *in vivo*. On the other hand, a previous report showed that global ischemia induces NRSF expression in the hippocampus, thereby causing repressive chromatin environments around the MOP-NRSE (Calderone et al., 2003; Formisano et al., 2007). However, the authors did not provide direct evidence that NRSF is responsible for MOP downregulation after ischemia, for example by NRSF knockdown.

As multiple promoters regulate NRSF gene expression (Koenigsberger et al., 2000), we analyzed promoter-specific transcription. The exon II-containing NRSF transcript, which is most active in neuronal cells (Koenigsberger et al., 2000), was found to be most responsive to nerve injury. Moreover, this increased transcription was predominantly associated with histone H4, but not H3, hyperacetylation at NRSF promoter II. These results are likely to be consistent with the pioneering report showing that NRSF expression is repressed at transcriptional level by HDAC-mediated mechanisms in mature neuron (Ballas et al., 2005). However, the regulatory mechanisms underlying nerve injury-induced epigenetic upregulation of NRSF in the DRG neurons remain elusive. Considering that NRSF expression is regulated by neuronal activity (Roopra et al., 2001), one possible mechanism underlying aberrant NRSF expression after nerve injury is the nerve injury-induced, long-lasting increase in ectopic activities of both C- and A-fibers (Xie et al., 2005). Neuronal activity regulates gene expression through extracellular signal-regulated kinase (ERK) activation (Ji and Woolf, 2001), a pathway that can lead to the activation of AP-1 and Sp1 (Karin, 1995; Barre et al., 2006), which putatively bind to the NRSF promoter II (Koenigsberger et al., 2000). Future studies should examine whether neuronal activity-induced ERK activation contributes to NRSF induction after nerve injury.

It has been assumed that the long-lasting alterations in pain-related gene expressions underlie the mechanisms of nerve injury-induced neuropathic pain (Devor, 2006; Hökfelt et al., 2006; Ueda, 2006). A unique example is a downregulation of $Na_v1.8$ expression in C-fiber neurons (Waxman et al., 1999; Ueda, 2006). Although $Na_v1.8$ gene is reported to contain putative NRSE (Otto et al., 2007), the transcriptional functions of $Na_v1.8$-NRSE remain unknown. As NRSE function is independent of its position and orientation (Kraner et al., 1992; Mori et al., 1992), it is likely that both the forward- and reverse-oriented $Na_v1.8$-NRSEs could act as a silencer. Indeed, we demonstrated that nerve injury causes NRSF binding and histone hypoacetylation at two putative $Na_v1.8$-NRSEs, and NRSF knockdown blocks nerve injury-induced $Na_v1.8$ downregulation. These results strongly suggest that these putative sites function as a silencer of $Na_v1.8$ gene expression in the DRG after nerve injury. In addition to MOP and $Na_v1.8$ genes, we have recently reported that NRSF plays a role in the nerve injury-induced epigenetic silencing of $K_v4.3$ gene, which has a NRSE sequence, in the DRG (Uchida et

al., 2010), although its functional role remains to be determined. On the other hand, the present study showed that NRSF causes TRPM8 and TRPA1, but not CGRP, downregulations in the DRG after nerve injury, although the putative NRSE sequences in these genes have low TFSEARCH scores. Further studies are required to elucidate the mechanisms for NRSF-directed silencing of TRPM8 and TRPA1 genes after nerve injury.

Epigenetic control, which includes DNA methylation and histone modifications such as acetylation and methylation, alters the accessibility of transcriptional machinery to DNA, thereby regulating gene expression (Abel and Zukin, 2008). Histone acetylation is thought to positively regulate transcription through loosening the DNA–histone interactions (Renthal and Nestler, 2009). In the present study, we successfully demonstrated that long-lasting upregulation of NRSF gene expression following nerve injury is correlated to the histone acetylation located adjacent to NRSF promoter II. Considering that NRSF gene expression is known to be positively regulated by neuronal activity (Roopra et al., 2001), it is suggested that sustained excitation of primary afferent neurons following nerve injury (Xie et al., 2005) may lead to the long-lasting upregulation of NRSF. As NRSF binds to NRSE and represses transcription by recruiting HDAC to induce hypoacetylation of histones (Ballas and Mandel, 2005), its long-lasting upregulation may in turn cause the continued downregulation of target genes in the DRG. Alternatively, the continued downregulation may be related to the fact that histone acetylation links to more stable epigenetic modifications, such as histone methylation and DNA methylation (Abel and Zukin, 2008; Renthal and Nestler, 2009).

Nerve injury abolished the peripheral morphine analgesia, possibly through a downregulation of MOP, whose expression in C-fiber neurons (Rashid et al., 2004) is negatively regulated by NRSF. The NRSF knockdown reversed the loss of peripheral morphine analgesia, suggesting that NRSF is crucial for pharmacological dysfunction of C-fibers in neuropathic pain. The morphine resistance accompanied by MOP downregulation in the DRG is also observed in the case with postherpetic neuralgia and bone cancer pain conditions (Takasaki et al., 2006; Yamamoto et al., 2008), although it remains to be determined whether NRSF-mediated epigenetic mechanisms also occur in these different types of chronic pain. In the

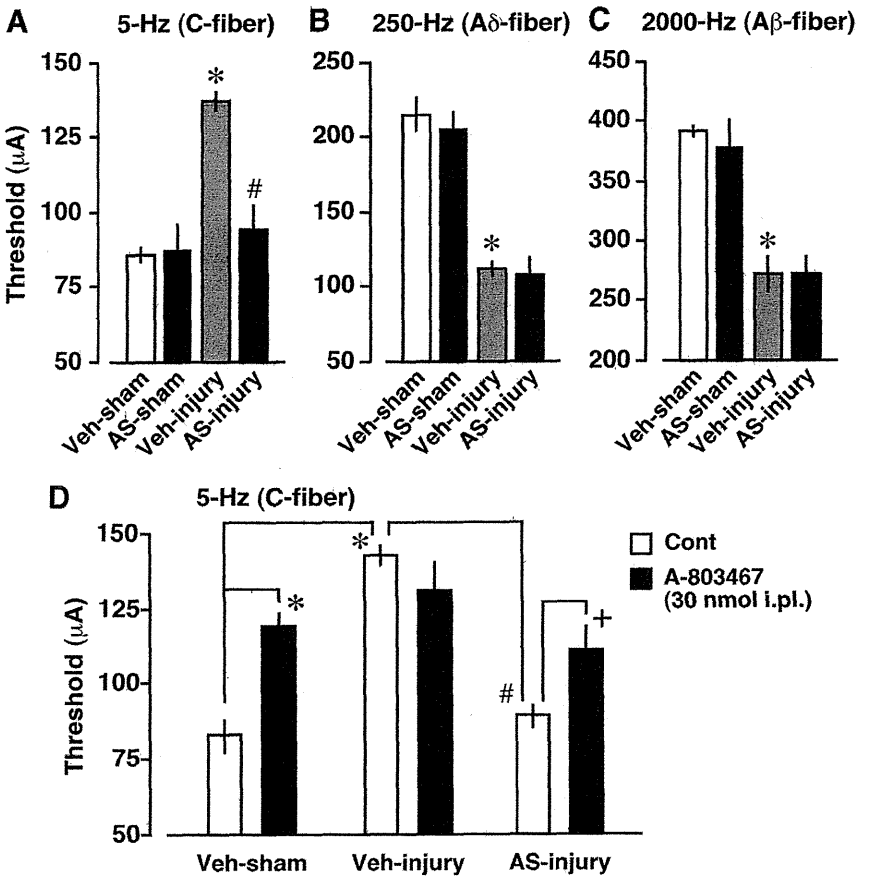

Figure 5. Blockade of nerve injury-induced C-fiber hypoesthesia and loss of peripheral A-803467 hypoesthesia by NRSF knockdown. ***A–C***, Blockade of nerve injury-induced hypoesthesia of C-fiber (5 Hz) (***A***), but not hypersensitization of Aδ-fiber (250 Hz) (***B***) and Aβ-fiber (2000 Hz) (***C***) by NRSF AS-ODN. Paw withdrawal thresholds to electrical stimulation (μA) were measured using the EPW test. $^{*}p < 0.05$ versus vehicle (Veh)-treated and sham-operated groups and $^{\#}p < 0.05$ versus Veh-treated and nerve-injured groups. ***D***, Recovery of nerve injury-induced loss of peripheral A-803467 hypoesthesia by AS-ODN. The C-fiber responses were assessed 30 min after intraplantar injection of control (Cont) or A-803467 (30 nmol). $^{*}p < 0.05$ versus Veh-treated, sham-operated, and Cont-treated groups. $^{\#}p < 0.05$ versus Veh-treated, nerve-injured, and Cont-treated groups. $^{+}p < 0.05$ versus AS-ODN-treated, nerve-injured, and Cont-treated groups. Data represent the means ± SEM from at least three mice.

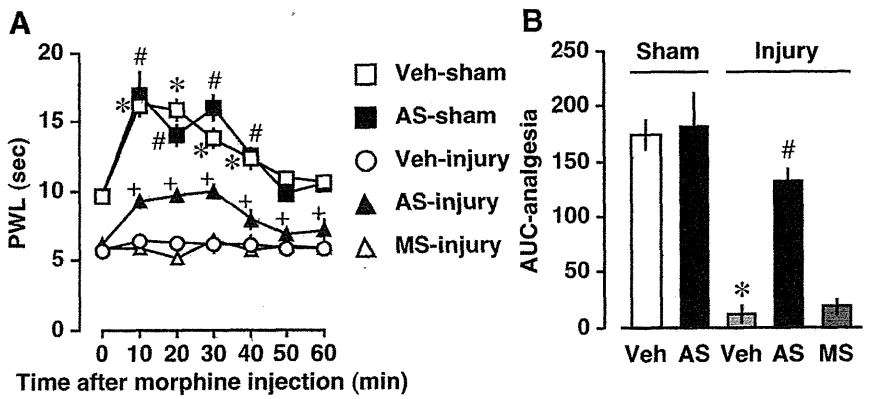

Figure 6. Blockade of nerve injury-induced loss of peripheral morphine analgesia by NRSF knockdown. Thermal pain threshold was assessed at day 7 postinjury by using a thermal paw withdrawal test. ***A***, Time course of thermal paw withdrawal latencies (PWL, in seconds) after morphine (30 nmol, intraplantar) injection. $^{*}p$, $^{\#}p$, or $^{+}p < 0.05$ versus corresponding 0 min, respectively. ***B***, Comparison of morphine analgesia by area under the curve (AUC). $^{*}p < 0.05$ versus vehicle (Veh)-treated and sham-operated groups and $^{\#}p < 0.05$ versus Veh-treated and nerve-injured groups. Data are expressed as the means ± SEM from at least four mice.

present study, we also demonstrated that the peripheral administration of A-803467 produces C-fiber-selective hypoesthesia in naive mice, possibly through a blockade of $Na_v1.8$, whose expression in C-fiber neurons (Waxman et al., 1999) is negatively regulated by NRSF. As seen in the case with morphine analgesia, the NRSF knockdown also reversed the nerve injury-induced loss of peripheral A-803467 hypoesthesia, being consistent with the recovery of $Na_v1.8$ gene expression. Of interest are the findings that NRSF knockdown has no effects on Aδ- and Aβ-hypersensitization, thermal hyperalgesia, and mechanical allodynia after nerve injury. These results are consistent with the report that the ablation of nociceptor neurons expressing $Na_v1.8$ has no effects on neuropathic hyperalgesia, assessed only by thermal and mechanical nociception tests (Abrahamsen et al., 2008). On the other hand, we also demonstrated that NRSF knockdown reverses the nerve injury-induced downregulation of TRPM8 and TRPA1, which have been proposed to function as cold receptors (Levine and Alessandri-Haber, 2007), although their TFSEARCH scores for NRSE are not high enough. It would be an interesting subject to examine whether NRSF-directed TRPM8 and TRPA1 downregulations are crucial for cold hypoesthesia, which is a negative symptom of neuropathic pain as seen in the clinical studies (Devigili et al., 2008; Leffler and Hansson, 2008).

In conclusion, the present study demonstrated that NRSF-directed epigenetic gene silencing of $Na_v1.8$ and MOP genes in the DRG is responsible for pathological and pharmacological dysfunctions of C-fiber after nerve injury. Elucidation of regulatory mechanisms for NRSE-NRSF systems after nerve injury might provide novel therapeutic targets for the unmet negative symptoms in neuropathic pain.

References

Abel T, Zukin RS (2008) Epigenetic targets of HDAC inhibition in neurodegenerative and psychiatric disorders. Curr Opin Pharmacol 8:57–64.

Abrahamsen B, Zhao J, Asante CO, Cendan CM, Marsh S, Martinez-Barbera JP, Nassar MA, Dickenson AH, Wood JN (2008) The cell and molecular basis of mechanical, cold, and inflammatory pain. Science 321:702–705.

Akopian AN, Souslova V, England S, Okuse K, Ogata N, Ure J, Smith A, Kerr BJ, McMahon SB, Boyce S, Hill R, Stanfa LC, Dickenson AH, Wood JN (1999) The tetrodotoxin-resistant sodium channel SNS has a specialized function in pain pathways. Nat Neurosci 2:541–548.

Ballas N, Mandel G (2005) The many faces of REST oversee epigenetic programming of neuronal genes. Curr Opin Neurobiol 15:500–506.

Ballas N, Grunseich C, Lu DD, Speh JC, Mandel G (2005) REST and its corepressors mediate plasticity of neuronal gene chromatin throughout neurogenesis. Cell 121:645–657.

Baron R (2006) Mechanisms of disease: neuropathic pain–a clinical perspective. Nat Clin Pract Neurol 2:95–106.

Barre L, Venkatesan N, Magdalou J, Netter P, Fournel-Gigleux S, Ouzzine M (2006) Evidence of calcium-dependent pathway in the regulation of human beta1,3-glucuronosyltransferase-1 (GlcAT-I) gene expression: a key enzyme in proteoglycan synthesis. FASEB J 20:1692–1694.

Borrelli E, Nestler EJ, Allis CD, Sassone-Corsi P (2008) Decoding the epigenetic language of neuronal plasticity. Neuron 60:961–974.

Bruce AW, Donaldson IJ, Wood IC, Yerbury SA, Sadowski MI, Chapman M, Gottgens B, Buckley NJ (2004) Genome-wide analysis of repressor element 1 silencing transcription factor/neuron-restrictive silencing factor (REST/NRSF) target genes. Proc Natl Acad Sci U S A 101:10458–10463.

Calderone A, Jover T, Noh KM, Tanaka H, Yokota H, Lin Y, Grooms SY, Regis R, Bennett MV, Zukin RS (2003) Ischemic insults derepress the gene silencer REST in neurons destined to die. J Neurosci 23:2112–2121.

Caspani O, Zurborg S, Labuz D, Heppenstall PA (2009) The contribution of TRPM8 and TRPA1 channels to cold allodynia and neuropathic pain. PLoS One 4:e7383.

Cheng HT, Dauch JR, Hayes JM, Hong Y, Feldman EL (2009) Nerve growth factor mediates mechanical allodynia in a mouse model of type 2 diabetes. J Neuropathol Exp Neurol 68:1229–1243.

Chong JA, Tapia-Ramirez J, Kim S, Toledo-Aral JJ, Zheng Y, Boutros MC, Altshuller YM, Frohman MA, Kraner SD, Mandel G (1995) REST: a mammalian silencer protein that restricts sodium channel gene expression to neurons. Cell 80:949–957.

Costigan M, Scholz J, Woolf CJ (2009) Neuropathic pain: a maladaptive response of the nervous system to damage. Annu Rev Neurosci 32:1–32.

Devigili G, Tugnoli V, Penza P, Camozzi F, Lombardi R, Melli G, Broglio L, Granieri E, Lauria G (2008) The diagnostic criteria for small fibre neuropathy: from symptoms to neuropathology. Brain 131:1912–1925.

Devor M (2006) Response of nerves to injury in relation to neuropathic pain. In: Wall and Melzack's textbook of pain (McMahon SB, Koltzenburg M, eds), pp 905–927. Oxford: Churchill Livingstone.

Dickenson A, Kieffer B (2006) Opiates: basic mechanisms. In: Wall and Melzack's textbook of pain (McMahon SB, Koltzenburg M, eds), pp 427–442. Oxford: Churchill Livingstone.

Fields HL, Rowbotham M, Baron R (1998) Postherpetic neuralgia: irritable nociceptors and deafferentation. Neurobiol Dis 5:209–227.

Formisano L, Noh KM, Miyawaki T, Mashiko T, Bennett MV, Zukin RS (2007) Ischemic insults promote epigenetic reprogramming of mu opioid receptor expression in hippocampal neurons. Proc Natl Acad Sci U S A 104:4170–4175.

Hargreaves K, Dubner R, Brown F, Flores C, Joris J (1988) A new and sensitive method for measuring thermal nociception in cutaneous hyperalgesia. Pain 32:77–88.

Hökfelt T, Zhang X, Xu XJ, Wiesenfeld-Hallin Z (2006) Central consequences of peripheral nerve damage. In: Wall and Melzack's textbook of pain (McMahon SB, Koltzenburg M, eds), pp 947–959. Oxford: Churchill Livingstone.

Inoue M, Rashid MH, Fujita R, Contos JJ, Chun J, Ueda H (2004) Initiation of neuropathic pain requires lysophosphatidic acid receptor signaling. Nat Med 10:712–718.

Jarvis MF, Honore P, Shieh CC, Chapman M, Joshi S, Zhang XF, Kort M, Carroll W, Marron B, Atkinson R, Thomas J, Liu D, Krambis M, Liu Y, McGaraughty S, Chu K, Roelofts, Zhong C, Mikusa JP, Hernandez G, et al. (2007) A-803467, a potent and selective Nav1.8 sodium channel blocker, attenuates neuropathic and inflammatory pain in the rat. Proc Natl Acad Sci U S A 104:8520–8525.

Ji RR, Woolf CJ (2001) Neuronal plasticity and signal transduction in nociceptive neurons: implications for the initiation and maintenance of pathological pain. Neurobiol Dis 8:1–10.

Karin M (1995) The regulation of AP-1 activity by mitogen-activated protein kinases. J Biol Chem 270:16483–16486.

Kim CS, Hwang CK, Choi HS, Song KY, Law PY, Wei LN, Loh HH (2004) Neuron-restrictive silencer factor (NRSF) functions as a repressor in neuronal cells to regulate the mu opioid receptor gene. J Biol Chem 279:46464–46473.

Klein JP, Tendi EA, Dib-Hajj SD, Fields RD, Waxman SG (2003) Patterned electrical activity modulates sodium channel expression in sensory neurons. J Neurosci Res 74:192–198.

Koenigsberger C, Chicca JJ 2nd, Amoureux MC, Edelman GM, Jones FS (2000) Differential regulation by multiple promoters of the gene encoding the neuron-restrictive silencer factor. Proc Natl Acad Sci U S A 97:2291–2296.

Koga K, Furue H, Rashid MH, Takaki A, Katafuchi T, Yoshimura M (2005) Selective activation of primary afferent fibers evaluated by sine-wave electrical stimulation. Mol Pain 1:13.

Kohno T, Ji RR, Ito N, Allchorne AJ, Befort K, Karchewski LA, Woolf CJ (2005) Peripheral axonal injury results in reduced mu opioid receptor pre- and post-synaptic action in the spinal cord. Pain 117:77–87.

Kraner SD, Chong JA, Tsay HJ, Mandel G (1992) Silencing the type II sodium channel gene: a model for neural-specific gene regulation. Neuron 9:37–44.

Kubat NJ, Amelio AL, Giordani NV, Bloom DC (2004) The herpes simplex virus type 1 latency-associated transcript (LAT) enhancer/rcr is hyperacetylated during latency independently of LAT transcription. J Virol 78:12508–12518.

Leffler AS, Hansson P (2008) Painful traumatic peripheral partial nerve injury-sensory dysfunction profiles comparing outcomes of bedside examination and quantitative sensory testing. Eur J Pain 12:397–402.

Levine JD, Alessandri-Haber N (2007) TRP channels: targets for the relief of pain. Biochim Biophys Acta 1772:989–1003.

Malmberg AB, Basbaum AI (1998) Partial sciatic nerve injury in the mouse

as a model of neuropathic pain: behavioral and neuroanatomical correlates. Pain 76:215–222.
Matsumoto M, Inoue M, Hald A, Xie W, Ueda H (2006) Inhibition of paclitaxel-induced A-fiber hypersensitization by gabapentin. J Pharmacol Exp Ther 318:735–740.
Matsumoto M, Xie W, Ma L, Ueda H (2008) Pharmacological switch in Abeta-fiber stimulation-induced spinal transmission in mice with partial sciatic nerve injury. Mol Pain 4:25.
Mori N, Schoenherr C, Vandenbergh DJ, Anderson DJ (1992) A common silencer element in the SCG10 and type II Na+ channel genes binds a factor present in nonneuronal cells but not in neuronal cells. Neuron 9:45–54.
Mori N, Mizuno T, Murai K, Nakano I, Yamashita H (2002) Effect of age on the gene expression of neural-restrictive silencing factor NRSF/REST. Neurobiol Aging 23:255–262.
Otto SJ, McCorkle SR, Hover J, Conaco C, Han JJ, Impey S, Yochum GS, Dunn JJ, Goodman RH, Mandel G (2007) A new binding motif for the transcriptional repressor REST uncovers large gene networks devoted to neuronal functions. J Neurosci 27:6729–6739.
Palm K, Belluardo N, Metsis M, Timmusk T (1998) Neuronal expression of zinc finger transcription factor REST/NRSF/XBR gene. J Neurosci 18:1280–1296.
Qiang M, Rani CS, Ticku MK (2005) Neuron-restrictive silencer factor regulates the *N*-methyl-D-aspartate receptor 2B subunit gene in basal and ethanol-induced gene expression in fetal cortical neurons. Mol Pharmacol 67:2115–2125.
Rashid MH, Inoue M, Kondo S, Kawashima T, Bakoshi S, Ueda H (2003) Novel expression of vanilloid receptor 1 on capsaicin-insensitive fibers accounts for the analgesic effect of capsaicin cream in neuropathic pain. J Pharmacol Exp Ther 304:940–948.
Rashid MH, Inoue M, Toda K, Ueda H (2004) Loss of peripheral morphine analgesia contributes to the reduced effectiveness of systemic morphine in neuropathic pain. J Pharmacol Exp Ther 309:380–387.
Renthal W, Nestler EJ (2009) Histone acetylation in drug addiction. Semin Cell Dev Biol 20:387–394.
Roopra A, Huang Y, Dingledine R (2001) Neurological disease: listening to gene silencers. Mol Interv 1:219–228.
Schoenherr CJ, Anderson DJ (1995) The neuron-restrictive silencer factor (NRSF): a coordinate repressor of multiple neuron-specific genes. Science 267:1360–1363.
Schoenherr CJ, Paquette AJ, Anderson DJ (1996) Identification of potential target genes for the neuron-restrictive silencer factor. Proc Natl Acad Sci U S A 93:9881–9886.
Staaf S, Oerther S, Lucas G, Mattsson JP, Ernfors P (2009) Differential regulation of TRP channels in a rat model of neuropathic pain. Pain 144:187–199.
Takasaki I, Nojima H, Shiraki K, Kuraishi Y (2006) Specific down-regulation of spinal mu-opioid receptor and reduced analgesic effects of morphine in mice with postherpetic pain. Eur J Pharmacol 550:62–67.
Taylor BK (2001) Pathophysiologic mechanisms of neuropathic pain. Curr Pain Headache Rep 5:151–161.
Uchida H, Sasaki K, Ma L, Ueda H (2010) Neuron-restrictive silencer factor causes epigenetic silencing of K(v)4.3 gene after peripheral nerve injury. Neuroscience 166:1–4.
Ueda H (2006) Molecular mechanisms of neuropathic pain-phenotypic switch and initiation mechanisms. Pharmacol Ther 109:57–77.
Ueda H (2008) Peripheral mechanisms of neuropathic pain-involvement of lysophosphatidic acid receptor-mediated demyelination. Mol Pain 4:11.
Waxman SG, Dib-Hajj S, Cummins TR, Black JA (1999) Sodium channels and pain. Proc Natl Acad Sci U S A 96:7635–7639.
Xie W, Strong JA, Meij JT, Zhang JM, Yu L (2005) Neuropathic pain: early spontaneous afferent activity is the trigger. Pain 116:243–256.
Yamamoto J, Kawamata T, Niiyama Y, Omote K, Namiki A (2008) Down-regulation of mu opioid receptor expression within distinct subpopulations of dorsal root ganglion neurons in a murine model of bone cancer pain. Neuroscience 151:843–853.
Zimmermann M (1983) Ethical guidelines for investigations of experimental pain in conscious animals. Pain 16:109–110.

Nagai et al. Molecular Pain 2010, 6:78
http://www.molecularpain.com/content/6/1/78

MOLECULAR PAIN

RESEARCH Open Access

Autotaxin and lysophosphatidic acid$_1$ receptor-mediated demyelination of dorsal root fibers by sciatic nerve injury and intrathecal lysophosphatidylcholine

Jun Nagai[1], Hitoshi Uchida[1], Yosuke Matsushita[1], Ryo yano[1], Mutsumi Ueda[1], Masami Niwa[2], Junken Aoki[3], Jerold Chun[4], Hiroshi Ueda[1*]

Abstract

Background: Although neuropathic pain is frequently observed in demyelinating diseases such as Guillain-Barré syndrome and multiple sclerosis, the molecular basis for the relationship between demyelination and neuropathic pain behaviors is poorly understood. Previously, we found that lysophosphatidic acid receptor (LPA_1) signaling initiates sciatic nerve injury-induced neuropathic pain and demyelination.

Results: In the present study, we have demonstrated that sciatic nerve injury induces marked demyelination accompanied by myelin-associated glycoprotein (MAG) down-regulation and damage of Schwann cell partitioning of C-fiber-containing Remak bundles in the sciatic nerve and dorsal root, but not in the spinal nerve. Demyelination, MAG down-regulation and Remak bundle damage in the dorsal root were abolished in LPA_1 receptor-deficient (*Lpar1*$^{-/-}$) mice, but these alterations were not observed in sciatic nerve. However, LPA-induced demyelination in *ex vivo* experiments was observed in the sciatic nerve, spinal nerve and dorsal root, all which express LPA_1 transcript and protein. Nerve injury-induced dorsal root demyelination was markedly attenuated in mice heterozygous for autotaxin (*atx*$^{+/-}$), which converts lysophosphatidylcholine (LPC) to LPA. Although the addition of LPC to *ex vivo* cultures of dorsal root fibers in the presence of recombinant ATX caused potent demyelination, it had no significant effect in the absence of ATX. On the other hand, intrathecal injection of LPC caused potent dorsal root demyelination, which was markedly attenuated or abolished in *atx*$^{+/-}$ or *Lpar1*$^{-/-}$ mice.

Conclusions: These results suggest that LPA, which is converted from LPC by ATX, activates LPA_1 receptors and induces dorsal root demyelination following nerve injury, which causes neuropathic pain.

Background

A significant amount of clinical evidence suggests that many demyelinating diseases are accompanied by neuropathic pain such as hyperalgesia (exaggerated pain sensations in response to mildly noxious stimuli) and allodynia (pain perception upon innocuous tactile stimuli), as seen in Guillain-Barré syndrome and multiple sclerosis[1,2]. Consistent with these clinical observations, peripheral demyelination is accompanied with thermal hyperalgesia and mechanical allodynia in *Prx* gene-deficient mice, which encodes for myelin protein in the peripheral nervous system [3]. On the other hand, there are many reports that experimental demyelination of peripheral or central neurons causes neuropathic pain behaviors [4-7].

Recently, we have reported that both neuropathic pain and demyelination are caused by sciatic nerve injury via a common pathway through LPA_1 receptors and its downstream RhoA/Rho kinase cascade [8]. In that report, intrathecal injection of LPA was found to mimic sciatic nerve injury. This finding was supported by a recent study, in which intratrigeminal injection of LPA causes neuropathic pain-like behaviors and demyelination in rats [7]. Direct evidence for LPA-induced demyelination

* Correspondence: ueda@nagasaki-u.ac.jp
[1]Division of Molecular Pharmacology and Neuroscience, Nagasaki University Graduate School of Biomedical Sciences, 1-14 Bunkyo-machi, Nagasaki 852-8521, Japan
Full list of author information is available at the end of the article

has been obtained in *ex vivo* cultures of primary afferent fibers [9]. Our recent study revealed that nerve injury-induced production of LPA through the action of autotaxin (ATX), which has lysophospholipase D activity and converts lysophosphatidylcholine (LPC) to LPA, is observed only in the spinal dorsal horn and dorsal root, but not in the spinal nerve, sciatic nerve and DRG for several hours [10]. Furthermore, we demonstrated that the injury-induced synthesis of LPC and subsequent conversion to LPA are both involved in the development of neuropathic pain [10,11]. However, the relationship of LPA production and demyelination following nerve injury remains to be determined. In the present study, we report that LPA_1 receptor-mediated demyelination following nerve injury selectively occurs at the dorsal root, as seen in LPA production. In addition, we found that LPC-induced demyelination is attributed to the effects of LPA, which is converted from LPC by ATX.

Methods

Animals

Male mutant mice for the *lpa1* gene (*Lpar1*$^{-/-}$) [12], *atx* $^{+/-}$ mice [13] and their sibling wild-type (WT) mice from the same genetic background (C57BL/6J), weighing 20-24 g, were used. They were housed at room temperature (21 ± 2°C) with free access to a standard laboratory diet and tap water. All procedures were approved by the Nagasaki University Animal Care Committee and complied with the recommendations of the International Association for the Study of Pain [14].

Surgery and tissue preparation

Partial ligation of the sciatic nerve was performed under pentobarbital (50 mg/kg) anesthesia, following the methods of Malmberg and Basbaum [15]. Briefly, the sciatic nerve of the right limb was exposed at the high thigh of level through a small incision, and the dorsal one half of the nerve thickness at the middle part of the sciatic nerve was tightly ligated with a silk suture. Sham surgery was performed similarly, except without touching the sciatic nerve. For the electron microscopy and toluidine blue staining, three different regions of peripheral nerve, sciatic nerve and spinal nerve at 1 - 2 and 15 mm, respectively apart from the ligation site and dorsal root within 10 mm proximal to the spinal cord at the level of L4-L6 were used. For the Western blot analysis, 5 mm-long sciatic nerve including ligature site, 5 mm-long spinal nerve 13 - 18 mm apart from the ligature site and 5 mm-long dorsal root proximal to the spinal cord were isolated. Averaged wet weights of each preparation were approximately 1.0-1.5 mg.

Drug injection

LPA (1-oleoyl-2-hydroxy-sn-3-glycerol-3-phosphate) and LPC (L-α-lysophosphatidylcholine) were purchased from Sigma-Aldrich (St. Louis, MO, USA). These drugs were dissolved in artificial cerebrospinal fluid (artificial CSF: 125 mM NaCl, 3.8 mM KCl, 1.2 mM KH_2PO_4, 26 mM $NaHCO_3$, 10 mM glucose, pH7.4). The intrathecal injection was given into the space between spinal L5 and L6 segments according to the method of Hylden and Wilcox [16].

Toluidine blue staining and transmission electron microscopy (TEM)

Nerve fibers were fixed with 2.5% glutaraldehyde in 0.1 M phosphate buffer (pH 7.4) overnight at 4°C. The fixed fibers were postfixed with 2% osmium tetroxide for 1 h at 25°C, dehydrated in a graded alcohol series, and embedded in Epon812. Thin sections (1 μm) were cut from each block, stained with alkaline toluidine blue, and examined by light microscopy. Ultrathin sections (80 nm thick) were cut with an Ultracut S (Leica, Wien, Austria), and then stained with uranyl acetate and lead citrate for 30 and 5 min, respectively. The stained sections were observed under an electron microscope (JEM-1200EX; JEOL, Tokyo, Japan), as previously reported [8].

Immunohistochemical analysis

Mice were deeply anesthetized with pentobarbital (50 mg/kg), and perfused with potassium-free phosphate buffered saline (K^+-free PBS, pH 7.4), followed by 4% paraformaldehyde solution. Nerve fibers were isolated, postfixed for 3 h, and cryoprotected overnight in 25% sucrose solution. The samples were fast-frozen in cryoembedding compound on a mixture of ethanol and dry ice and stored at -80°C until ready for use. The fibers were cut on a cryostat at a thickness of 30 μm, thaw-mounted on silane-coated glass slides, and air-dried overnight at 25°C. The sections were incubated with blocking buffer containing anti-mouse IgG (1:100; Zymed, South San Francisco, CA, USA) and 4% bovine serum albumin in PBST (0.1% Triton X-100 in K^+-free PBS), and then reacted with anti-myelin-associated glycoprotein (MAG) antibody (1:1000; Chemicon, Temecula, CA, USA) overnight at 4°C. After washing, the sections were incubated with a secondary antibody, Alexa Fluor 488-conjugated anti-mouse IgG (1:300; Invitrogen, Eugene, Oregon, USA), for 3 h at 25°C. MAG-immunoreactivity was detected by automatic fluorescence microscopy using BZ Image Measurement software (Bio-Zero, Keyence, Tokyo, Japan).

Western blot analysis

According to the manufacturer's instructions, non-reduced protein was used for detection of MAG, and reduced protein was used for LPA_1 receptor and β-tubulin. Total protein (20 μg) was separated on SDS-polyacrylamide gels (12%). Primary antibodies were

used at the following dilutions: mouse anti-MAG antibody (1:1000), rabbit anti-LPA_1 receptor antibody (1:500) [17] and rabbit anti-β-tubulin polyclonal antibody (1:1000; Santa Cruz Biotechnology, Santa Cruz, CA, USA). Horseradish peroxidase-labeled anti-mouse IgG and horseradish peroxidase-labeled anti-rabbit IgG were used as a secondary antibody at a dilution of 1:1000. Immunoreactive bands were detected using an enhanced chemiluminescent substrate (SuperSignal West Pico Chemiluminescent Substrate; Pierce Chemical, Rockford, IL) for the detection of horseradish peroxidase.

Reverse-transcription polymerase chain reaction (RT-PCR)

Total RNA was extracted from L4-6 dorsal root ganglion (DRG), dorsal root, spinal nerve and sciatic nerve using TRIzol (Invitrogen, Carlsbad, CA, USA), and 1 μg of RNA was used for cDNA synthesis. The PCR primers used in the present study were as follows: for β-actin, 5'-AGGCTCTTTTCCAGCCTTCCT-3' (forward) and 5'-GTCTTTACGGATGTCAACGTCACA-3' (reverse); for LPA_1, 5'-ATCTTTGGCTATGTTCGCCA-3' (forward) and 5'-TTGCTGTGAACTCCAGCCA-3' (reverse). β-actin was used as an internal control. The cycling conditions for all primers were 2 min at 94°C, followed by 35 cycles of 45 sec at 94°C, 45 sec at 58°C and 70 sec at 72°C.

Ex vivo cultures of nerve fibers

Ex vivo cultures of nerve fibers were performed as described previously [9]. Briefly, nerve fibers with DRG were isolated and the spinal vertebrae were carefully removed. Nerve fibers were washed with ice-cold PBS (pH7.4) containing penicillin and streptomycin, and grown in Dulbecco's modified Eagle's medium without serum. The cultures were maintained at 37°C in the presence of 5% CO_2. LPA and LPC, used in *ex vivo* experiments, were dissolved in dimethyl sulfoxide to make a 20 mM stock solution that was stored at -80°C.

Statistical analysis

In vivo experiments, the differences between multiple groups were analyzed by one-way ANOVA with Scheffe's multiple comparison post-hoc analysis. In *ex vivo* experiments, the data were analyzed using Student's *t*-test. The criterion of significance was set at $^*p < 0.05$. All results are expressed as the mean ± SEM.

Results

LPA_1 receptor-dependent demyelination of dorsal root fiber

To quantify injury-induced demyelination in dorsal root, spinal nerve and sciatic nerve regions, we performed toluidine blue staining, as described previously [8,9]. As shown in Figure 1, marked demyelination was observed in the dorsal root and sciatic nerve, but not spinal nerve regions at day 7 after nerve injury. Demyelination in the dorsal root and sciatic nerve was characterized by swollen myelin, decrease in myelin thickness and loss of myelin. Significant demyelination was limited within the range of 1 - 2 mm apart from the ligation site. Quantitative analysis revealed that injury increases the incidence of demyelination to approximately 35% of total fibers in the dorsal root and 20% in the sciatic nerve, but not in the spinal nerve. When *Lpar1*$^{-/-}$ mice were used, demyelination was completely abolished in the dorsal root, but not in the sciatic nerve. However, injury did not increase the incidence of demyelination in the spinal nerve in both WT and *Lpar1*$^{-/-}$ mice.

To gather more information on the morphological alterations in the myelinated fibers after injury, we performed TEM analysis. This analysis also revealed that demyelination is observed in the dorsal root and sciatic nerve, but not in the spinal nerve at day 7 after nerve injury (Figure 2). As described previously [9], the myelinated fibers were divided into two types according to the diameter of the axon and the thickness of the myelin sheath as follows: Aβ-fiber (8-15 μm in diameter and 0.6-1.0 μm thick) and Aδ-fiber (3-6 μm in diameter and 0.4-0.6 μm thick). However, there was no clear difference in the incidence of demyelination between such characterized Aβ- and Aδ-fibers. In good agreement with data obtained from toluidine blue analysis, the injury-induced demyelination was absent in the dorsal root, but not in the sciatic nerve of *Lpar1*$^{-/-}$ mice (Figure 2). Taken together, these results strongly suggest that the LPA_1 receptor-dependent demyelination occurs only in the dorsal root, but not spinal nerve and sciatic nerve, after nerve injury. The sciatic nerve demyelination seems to be caused by local inflammation following nerve damage [18], which is unrelated to LPA_1 receptor-mediated neuropathic pain.

LPA_1 receptor-dependent damage of Remak bundles

C-fibers without a myelin sheath bunch such as Remak bundles, and each fiber in a bundle is partitioned by Schwann cells, as described previously [9]. In the TEM analysis, we found that injury causes some damage in the partitioning of C-fibers in the Remak bundle of the dorsal root and sciatic nerve, but not in the spinal nerve at day 7 post-injury, and this damage were abolished in the dorsal root of *Lpar1*$^{-/-}$ mice, but not in the sciatic nerve (Figure 3), being consistent with data obtained from demyelination studies (Figures 1 and 2).

LPA_1 receptor-dependent down-regulation of MAG protein expression

MAG, a minor component of myelin, plays a key role in the maintenance of myelin integrity [19,20]. In the

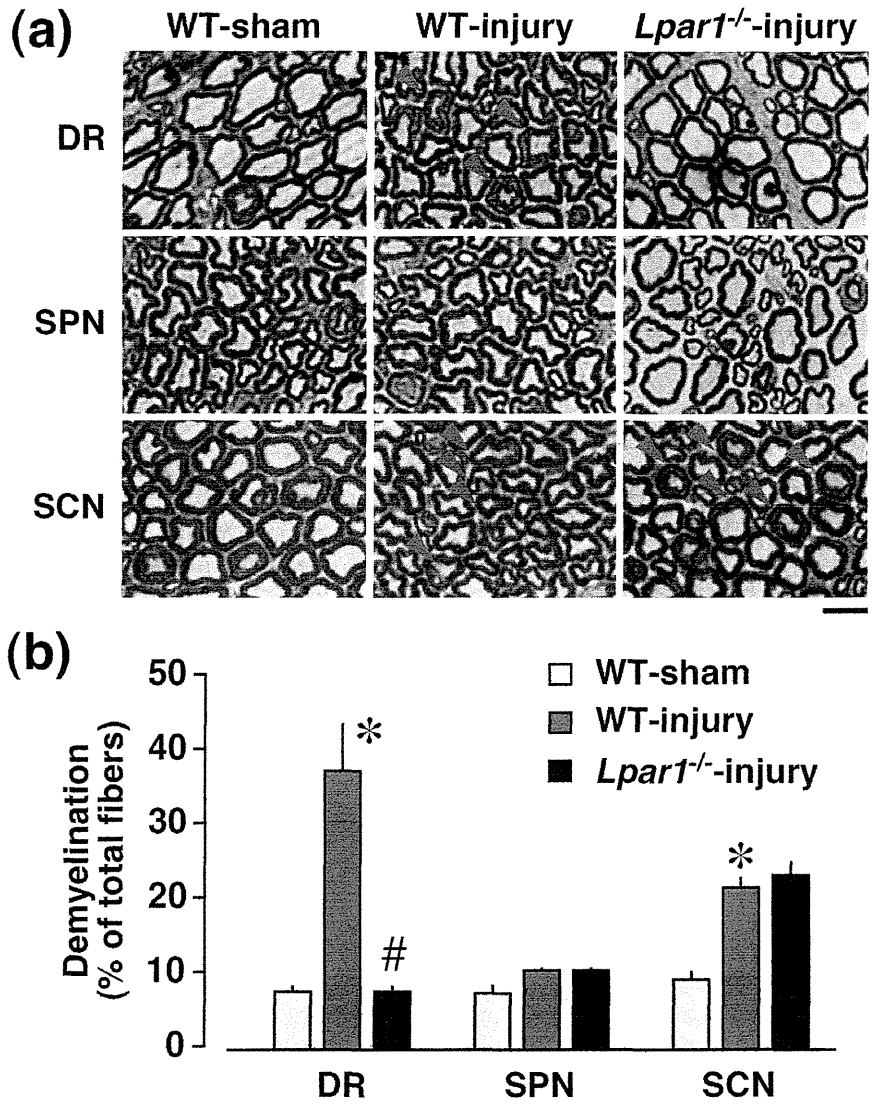

Figure 1 LPA_1 receptor-dependent and -independent demyelination after nerve injury in toluidine blue analysis. Toluidine blue analysis was performed at day 7 post-injury. (a) Representative photographs of DR (dorsal root), SPN (spinal nerve) and SCN (sciatic nerve) regions in WT or *Lpar1*$^{-/-}$ mice. Arrow indicates a demyelinated fiber. Scale bar, 10 μm. (b) Quantification of demyelinated fibers. Data are expressed as a percentage of total fibers in each region. *$p < 0.05$, *vs.* WT and sham-operated mice and #$p < 0.05$, *vs.* WT and nerve-injured mice. Results represent the mean ± SEM from 3-5 independent experiments.

peripheral nervous system, MAG expression has been found abundantly in paranodal regions and to a lesser extent in periaxonal Schwann cell membranes [21]. Strong MAG signals were found in paranodal regions, while weaker signals were detected along axons in the dorsal root, spinal nerve and sciatic nerve regions (Figure 4a). The MAG signals were down-regulated in the dorsal root and sciatic nerve, but not in the spinal nerve, at 7 day post-injury. Moreover, we found that injury-induced MAG down-regulation is completely blocked in the dorsal root of *Lpar1*$^{-/-}$ mice, but not in the sciatic nerve. Similar results were obtained by western blot analysis (Figure 4b). Quantitative analysis revealed that injury significantly induced down-regulation of MAG approximately 20% in the dorsal root (MAG/tubulin signals; 78.8 ± 3.8%/n = 8, compared to sham) and 30% in the sciatic nerve (67.0 ± 7.9%/n = 5), but not in the spinal nerve (109.3 ± 8.8%/n = 4). When *Lpar1*$^{-/-}$ mice were used, down-regulation of MAG was completely abolished in the dorsal root (104.1 ± 10.3%/n = 4), but not in the sciatic nerve (62.2 ± 10.7%/n = 5). However, injury did not decrease the intensity of MAG in the spinal nerve in both WT (109.3 ± 8.8%/n = 4) and *Lpar1*$^{-/-}$ mice (102.6 ± 6.2%/n = 4). Injury-induced

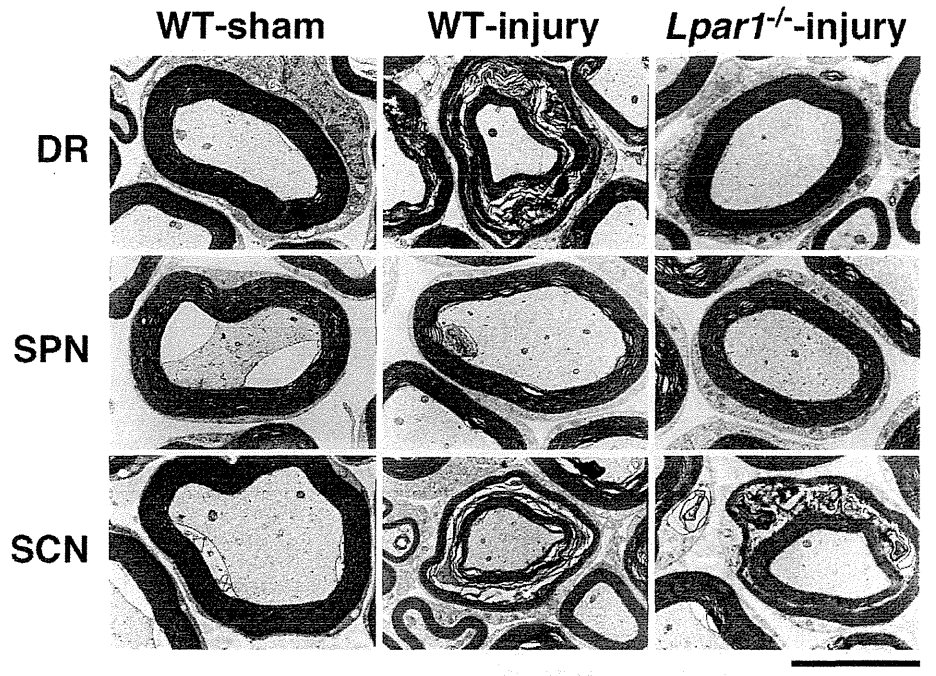

Figure 2 Analysis of LPA_1 receptor-dependent and -independent A-fiber demyelination by TEM analysis. TEM analysis was performed at day 7 post-injury. Photographs show representative data on A-fiber myelination in dorsal root (DR), spinal nerve (SPN) and sciatic nerve (SCN) fibers in WT or *Lpar1*$^{-/-}$ mice. Scale bar, 5 μm.

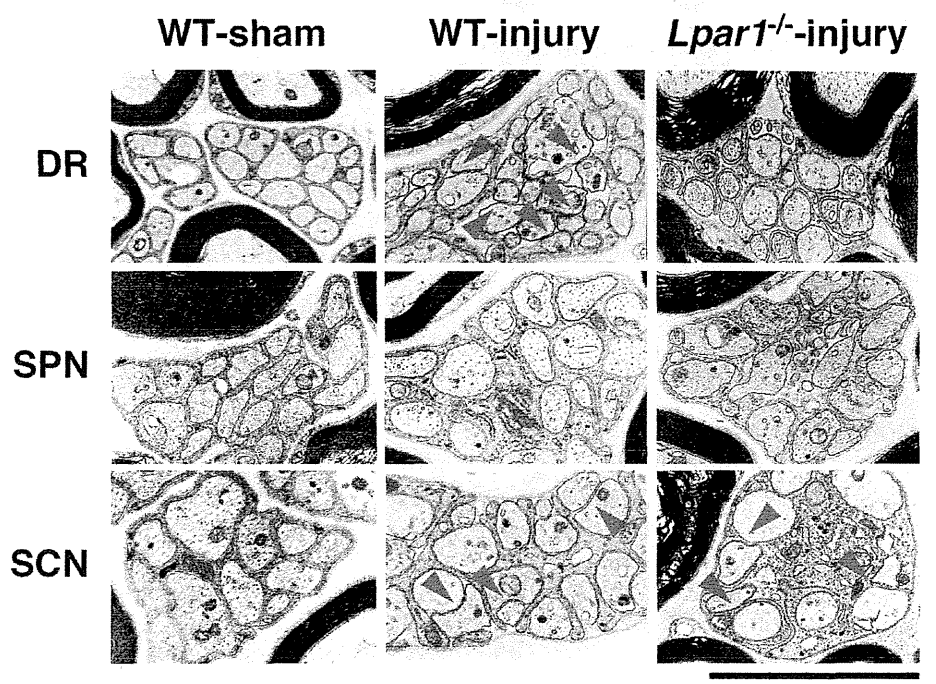

Figure 3 Analysis of LPA_1 receptor-dependent and -independent Remak bundle disruption by TEM. TEM analysis was performed at day 7 post-injury. Photographs show representative data on C-fiber-containing Remak bundles in dorsal root (DR), spinal nerve (SPN) and sciatic nerve (SCN) fibers in WT or *Lpar1*$^{-/-}$ mice. Arrow indicates a direct contact between C-fibers in the Remak bundle. Scale bar, 5 μm.

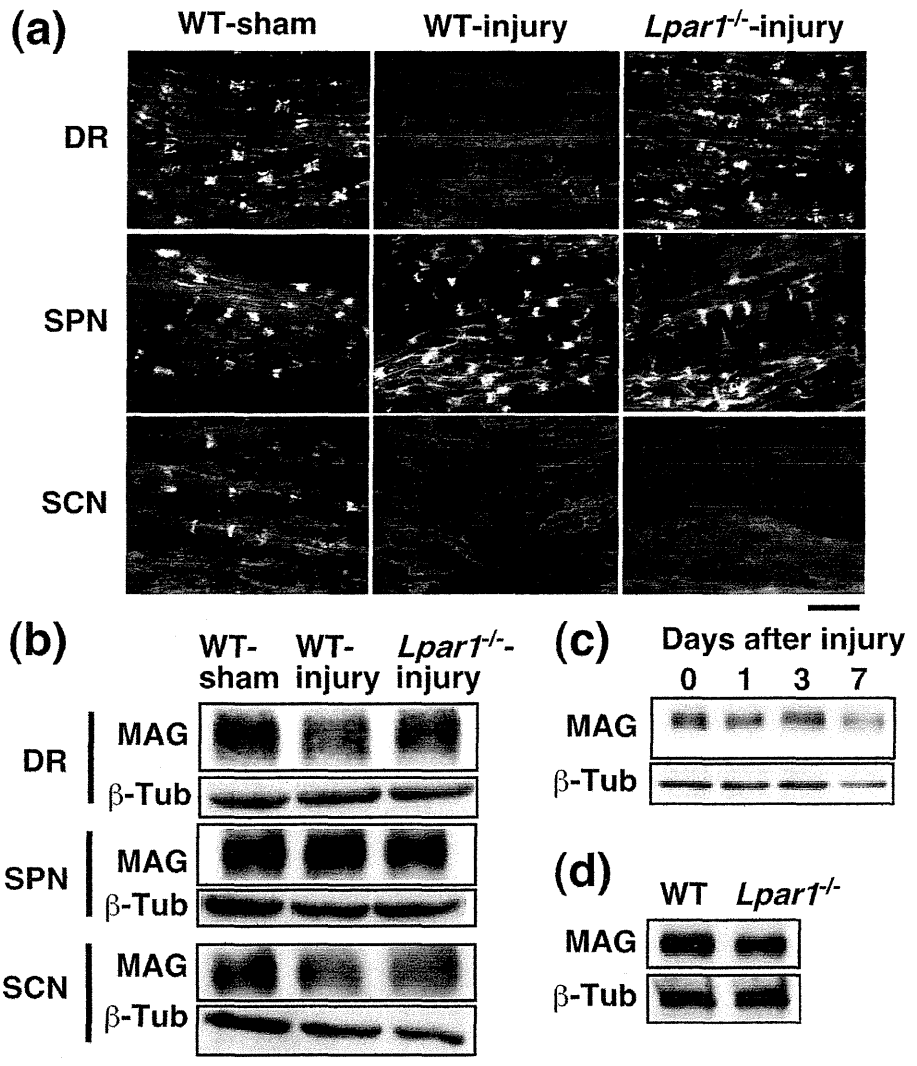

Figure 4 LPA_1 receptor-dependent and -independent down-regulation of MAG. (a and b) The MAG expression following nerve injury in the dosal root (DR), spinal nerve (SPN) and sciatic nerve (SCN) fibers in WT or *Lpar1*$^{-/-}$ mice at day 7 post-injury, were assessed by immunohistochemical analysis (a) and western blot analysis (b). (a) Photographs show representative data. Scale bar, 20 μm. (b) Immunoreactive signals for MAG (100 kDa) and β-tubulin (β-Tub; 55 kDa) were detected. (c) Time-course of MAG down-regulation in the dorsal root after injury. (d) Comparison of MAG expression levels between uninjured WT and *Lpar1*$^{-/-}$ mice. Photographs show a representative image of a western blot. Data were obtained from three independent experiments.

MAG down-regulation in the dorsal root was slightly observed at day 1 (91.1 ± 7.1%/n = 3) and day 3 (91.8 ± 6.5%/n = 3) post-injury (Figure 4c). On the other hand, there was no difference in the basal MAG expression level in the dorsal root regions between uninjured WT (100 ± 7.3%/n = 3) and *Lpar1*$^{-/-}$ mice (93.7 ± 5.6%/n = 3, compared to WT) (Figure 4d).

LPA-induced ex vivo demyelination in whole regions of sensory fibers

To assess the responsiveness of dorsal root, spinal nerve and sciatic nerve fibers to LPA, we performed *ex vivo* cultures of nerve fibers with DRG, as described previously [9]. Toluidine blue analysis revealed that addition of LPA (1 μM) to *ex vivo* cultures causes demyelination in all regions at 24 h post-treatment, though demyelination in the spinal nerve was weaker than others (Figure 5).

Previously, we have reported that the LPA_1 receptor-mediated Rho-Rho kinase pathway is crucial for LPA-induced demyelination [8]. Using RT-PCR analysis, however, we found that the LPA_1 receptor is ubiquitously expressed in the dorsal root, spinal nerve, sciatic nerve and DRG (Figure 6a). Western blot analysis also showed similar expression patterns of the LPA_1 receptor (Figure 6b).

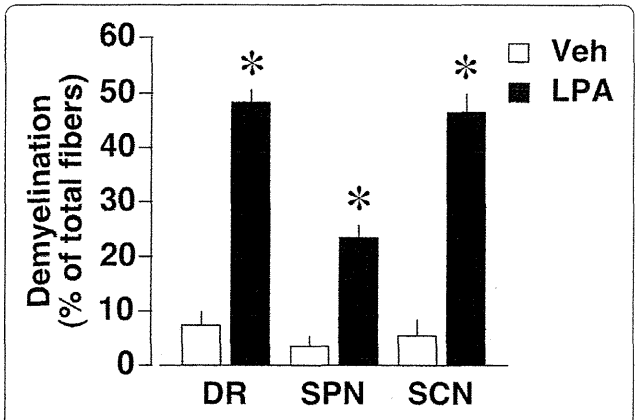

Figure 5 Susceptibility of dorsal root, spinal nerve and sciatic nerve fibers to LPA-induced demyelination in the *ex vivo* culture model. Toluidine blue analysis was performed at 24 h after the addition of LPA (1 μM) to the *ex vivo* culture of dorsal root (DR), spinal nerve (SPN) or sciatic nerve (SCN) fibers. Results are calculated as a percentage of total fibers in each region, and expressed as the mean ± SEM from 3-5 independent experiments. *$p < 0.05$, *vs.* vehicle (Veh)-treated groups.

ATX-mediated demyelination following injury

As ATX plays a key role in nerve injury-induced LPA production and neuropathic pain [10,11], we used *atx*$^{+/-}$ mice to examine the involvement of *de novo* synthesis of LPA in dorsal root demyelination. In the toluidine blue analysis, the injury-induced demyelination level in *atx*$^{+/-}$ mice was reduced to approximately half in WT mice (Figure 7), being consistent with the change of LPA production and neuropathic pain in *atx*$^{+/-}$ mice [10,11]. There was no significant difference in the morphology of myelinated fibers and basal incidence of demyelinated fibers between *atx*$^{+/-}$ and WT mice.

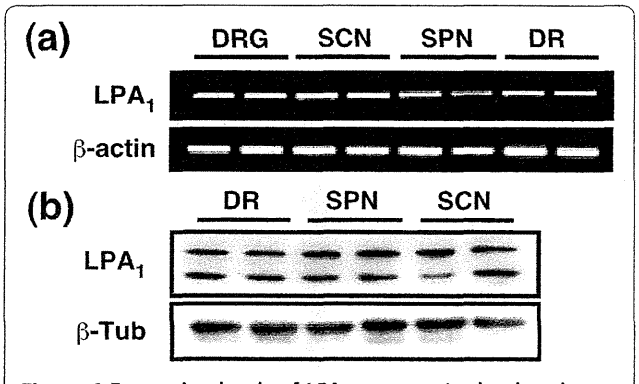

Figure 6 Expression levels of LPA_1 receptor in the dorsal root, spinal nerve and sciatic nerve fibers. (a) The mRNA expression levels of LPA_1 receptors in the dorsal root ganglion (DRG), dorsal root (DR), spinal nerve (SPN) or sciatic nerve (SCN) fibers *in vivo*, assessed by RT-PCR. β-actin was used as an internal control. Photographs show the representative image of RT-PCR. Data were obtained from three independent experiments. (b) Protein expression levels of LPA_1 receptors in the dorsal root (DR), spinal nerve (SPN) or sciatic nerve (SCN) fibers *in vivo*, using western blot analysis. β-tubulin (β-Tub) was used as an internal control. Photographs show the representative image of western blot. Data were obtained from three independent experiments.

LPC-induced ex vivo demyelination in the presence of ATX

Based on previous observations that LPC-induced neuropathic pain behaviors are abolished or markedly attenuated in *Lpar1*$^{-/-}$ or *atx*$^{+/-}$ mice, respectively [22], we examined the effects of LPC in the presence and absence of recombinant ATX on demyelination in *ex vivo* experiments. As shown in Figure 8, toluidine blue analysis revealed that LPC at a concentration as low as 100 ng/ml (approximately 0.2 μM) in the presence of ATX (30 ng/ml) markedly increases the incidence of demyelination of dorsal roots to 35% of total myelinated fibers, being equivalent to the level of *ex vivo* dorsal root demyelination by LPA (1 μM) treatment and

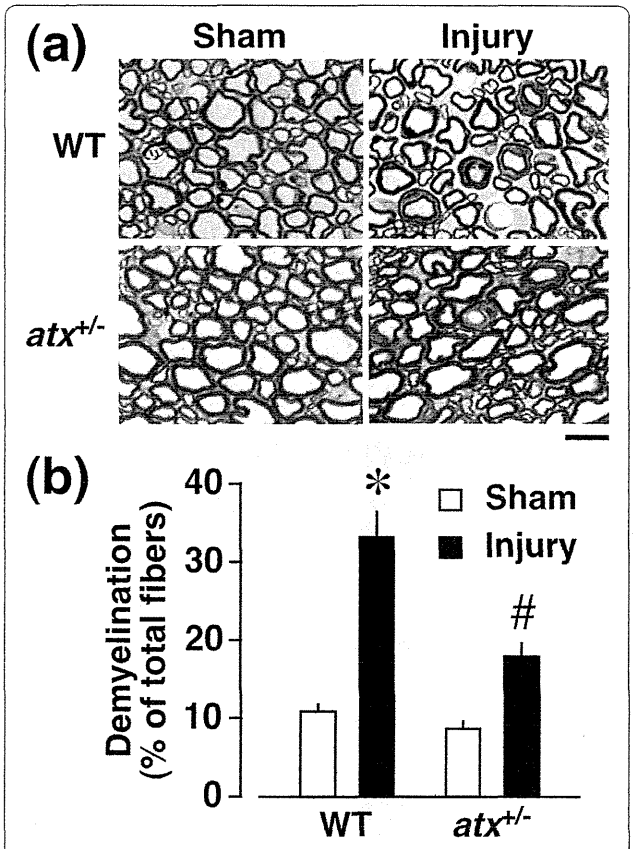

Figure 7 Attenuation of injury-induced dorsal root demyelination in *atx*$^{+/-}$ mice. Toluidine blue analysis was performed at day 7 post-injury in WT or *atx*$^{+/-}$ mice. (a) Photographs show representative data in the dorsal root. Scale bar, 10 μm. (b) Quantification of demyelinated fibers. Results are calculated as a percentage of total fibers, and expressed as the mean ± SEM from 3-5 independent experiments. *$p < 0.05$, *vs.* WT and sham-operated mice and #$p < 0.05$, *vs.* WT and nerve-injured mice.

in vivo dorsal root demyelination following nerve injury. There was no significant change in the extent of demyelination by LPC or ATX alone.

ATX- and LPA_1 receptor-mediated demyelination by LPC

When LPC (15 μg, approximately 30 nmol) was given intrathecally, there was an increase in dorsal root demyelination at day 4 post-injection. The level was approximately 30% (Figure 9), being equivalent to that (30%) by intrathecally administered 1 nmol of LPA [8]. The demyelination was significantly attenuated in $atx^{+/-}$ mice, and abolished in $Lpar1^{-/-}$ mice (Figure 9).

Discussion

Myelination is known to insulate nerve fibers for rapid nerve conduction. Demyelination is thought to reduce conduction velocity, thereby causing sensory and motor dysfunction in peripheral demyelinating diseases, including Charcot-Marie-Tooth disease [23]. However, there are reports that demyelination leads to neuronal hyperexcitability associated with neuropathic hyperalgesia and allodynia [3,4]. Thus, some secondary events after demyelination may be included in this functional difference *in vivo*. In agreement with these findings, the formation of electrical crosstalk (emphatic interaction) or sprouting after demyelination has been implicated in neuronal hyperexcitability [24-26].

In the present study, we found that nerve injury induces demyelination and damages Remak bundles in the dorsal root. These changes were abolished in $Lpar1^{-/-}$ mice, suggesting that LPA causes these changes via Schwann cells. Indeed, we have reported that the addition of LPA causes demyelination and damage of Remak bundles in dorsal root fibers in *ex vivo* culture experiments [9]. Regarding the molecular basis for demyelination, we have proposed that LPA down-regulates gene and protein expression of compact myelin proteins, such as myelin basic protein, peripheral myelin protein 22 and myelin protein zero [8,9]. Here, we further observed down-regulation of MAG, which inhibits nerve sprouting through regulation of actin assembly by the Rho-Rho kinase-Lim kinase pathway [24]. Indeed, MAG down-regulation following nerve injury is reported to induce axonal sprouting [27]. This action seems to be related to the challenging proposal that the synaptic reorganization involved in neuropathic allodynia may be mediated by axonal sprouting in the DH [24,28].

In the present study, we demonstrated that the sciatic nerve injury caused LPA_1 receptor-mediated demyelination and its underlying MAG down-regulation only in the dorsal root, but not spinal nerve or sciatic nerve (Figures 1, 2, 4). In the sciatic nerve, there was LPA_1-independent demyelination. However, as LPA-mediated *in vitro* (*ex vivo*) demyelination was observed all in dorsal root, spinal nerve and sciatic nerve (Figure 5), it seems that machineries required for LPA-mediated demyelination are present in these three regions. Therefore, the dorsal root-specific LPA_1-mediated demyelination would

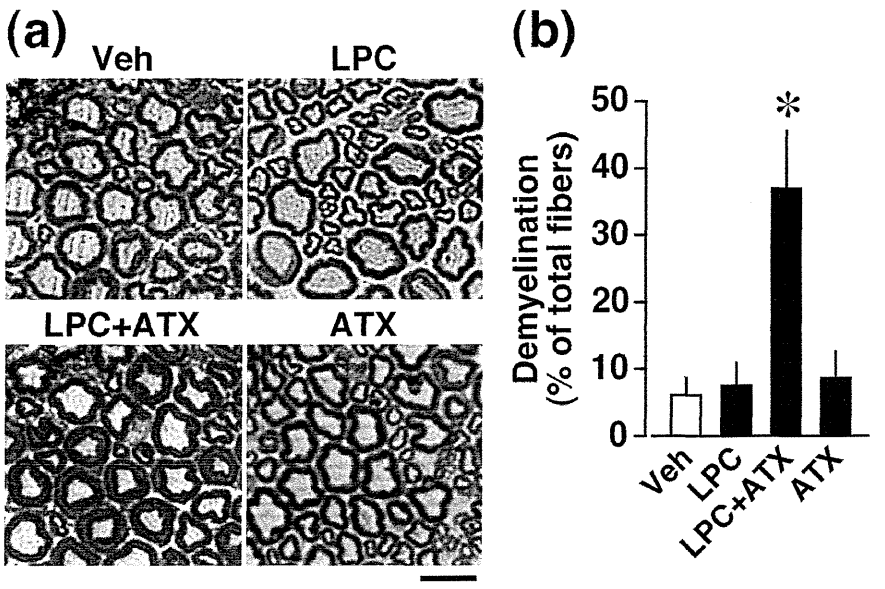

Figure 8 LPC-induced dorsal root demyelination mediated through ATX. Toluidine blue analysis was performed at 24 h after the addition of 100 ng/ml of LPC to *ex vivo* cultures of DR fibers in the presence or absence of ATX (30 ng/ml). (a) Photographs show representative data. Scale bar, 10 μm. (b) Quantification of demyelinated fibers. Results are calculated as a percentage of total fibers, and expressed as the mean ± SEM from 3-5 independent experiments. *$p < 0.05$, *vs.* vehicle (Veh)-treated group.

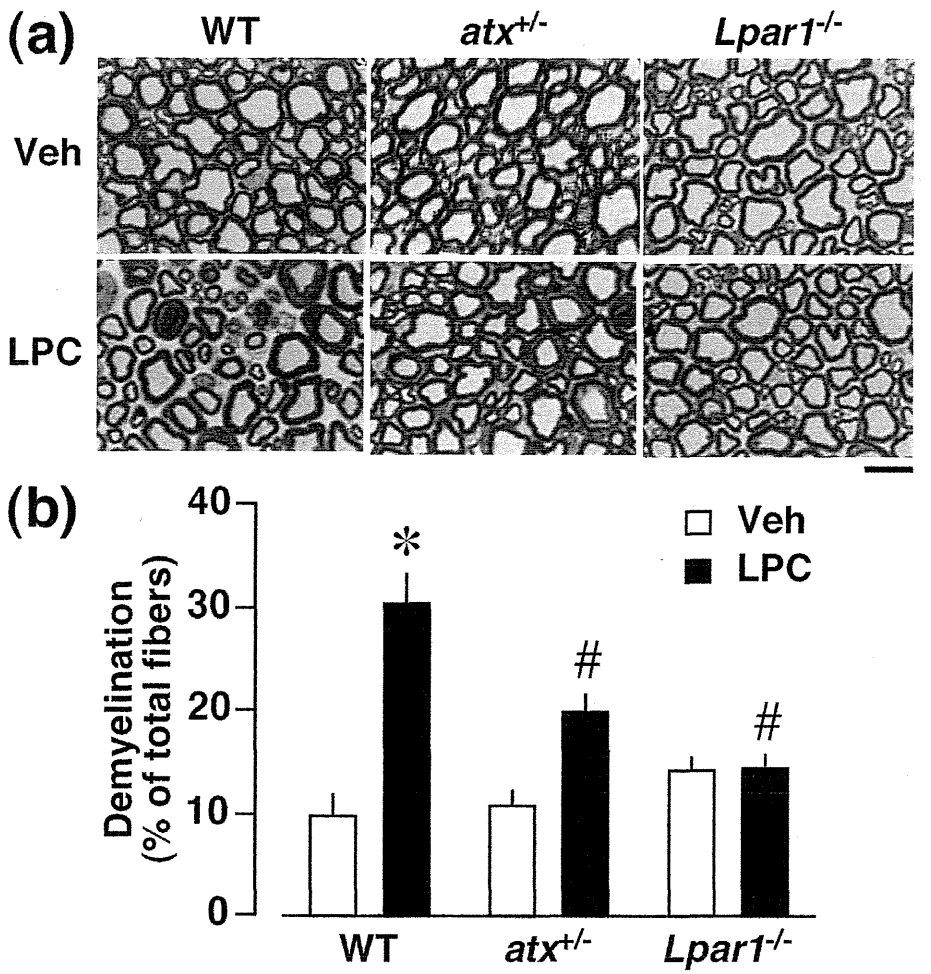

Figure 9 LPC-induced dorsal root demyelination mediated through ATX and LPA_1 receptors *in vivo*. Toluidine blue analysis was performed at day 4 after the intrathecal injection of LPC (15 μg) in WT, *atx*$^{+/-}$ or *Lpar1*$^{-/-}$ mice. (a) Photographs show representative data in the dorsal root. Scale bar, 10 μm. (b) Quantification of demyelinated fibers. Results are calculated as a percentage of total fibers, and expressed as the mean ± SEM from 3-5 independent experiments. *$p < 0.05$, *vs.* WT and vehicle (Veh)-treated mice and #$p < 0.05$, *vs.* WT and LPC-treated mice.

be explained by the speculation that LPA is produced in spinal cord and transferred to the dorsal root, where demyelination occurs. However, there is still a possibility that dorsal root demyelination is attributed to the action of LPA derived from dorsal root. Regarding the proposal that LPA involved in the dorsal root demyelination comes from the spinal dorsal horn, we have reported that the intense stimulation of spinal dorsal horn *in vitro* causes *de novo* production of LPA [29].

On the other hand, there are reports that demyelination at the nerve-injured site, is caused by an activation of matrix metalloproteinase-9 [30,31]. However, this activation is unlikely related to the action of LPA, since no significant LPA production in the sciatic nerve was observed by nerve injury [10]. Furthermore, metalloproteinase inhibition did not affect MAG down-regulation in the dorsal root following intrathecally administered LPA [32], which mimics the nerve injury in terms of induction of neuropathic pain and its underlying mechanisms [8].

The present study demonstrated that sciatic nerve injury did not cause demyelination in the spinal nerve. The partial ligation of sciatic nerve was performed within 1 mm-long fiber portion in sciatic nerve, and significant demyelination was limited within the range of 1 - 2 mm apart from the ligation site. As isolated spinal nerve region is over 10 mm apart from the ligation site of the sciatic nerve, it is unlikely that inflammatory effects in sciatic nerve, if any, affect on the spinal nerve region.

Accumulating evidence has shown that LPC, a precursor of LPA, induces focal demyelination, thereby causing neuropathic pain conditions [4,33]. These studies topically applied as much as 1-2% (10-20 μg/μl) of LPC to the nerve fibers, and this dose is reported to be toxic to myelinating cells due to the detergent-like properties of LPC [34]. On

the other hand, in the present study we observed that intrathecal administration of 0.3% (3 μg/μl, 5 μl) LPC, which in turn would be diluted by circulating CSF, causes dorsal root demyelination. In addition, LPC-induced demyelination was attenuated to approximately 50% in $atx^{+/-}$ mice and abolished in $Lpar1^{-/-}$ mice. Similar attenuation was observed in injury-induced demyelination in $atx^{+/-}$ mice, being consistent with the finding that injury-induced neuropathic pain and LPA production in the dorsal root are also attenuated to approximately 50% in $atx^{+/-}$ mice [10]. In the present study, we failed to detect any significant demyelination of nerve fibers in the *ex vivo* study with LPC, but further addition of recombinant ATX showed significant demyelination at equivalent levels to the case with LPA. The reason LPC did not cause demyelination, may be attributed to the loss of ATX throughout the isolation and preparation processes of dorsal root fibers in the *ex vivo* study, consistent with LPA production [29,35]. However, we have demonstrated that significant amounts of ATX (5 μg/mL) exist in CSF *in vivo* [29]. Thus, we have successfully provided evidence that demyelination occurs through the conversion of LPC into LPA by ATX *in vivo*.

Lastly, although the relationship between LPA- or injury-induced demyelination and development of neuropathic pain remains to be fully elucidated, we have recently observed that calpain inhibition abolishes down-regulation of MAG in the dorsal root and neuropathic pain after intrathecal administration of LPA or nerve injury [32]. However, further studies will clarify the role of demyelination underlying injury-induced neuropathic pain.

Conclusions

The present study demonstrated that LPA_1 receptor signaling following injury causes demyelination specifically at the dorsal root, which is consistent with *de novo* LPA production. In addition, we found that demyelination by topical application of LPC is attributed to the action of LPA after conversion by ATX.

List of abbreviations

ATX: autotaxin; $atx^{+/-}$: mice heterozygous for autotaxin; CSF: cerebrospinal fluid; DH: dorsal horn; DRG: dorsal root ganglion; GAPDH: glyceraldehyde-3-phosphate dehydrogenase; i.t.: intrathecal; LPA: lysophosphatidic acid; $Lpar1^{-/-}$: LPA_1 receptor-deficient mice; LPC: lysophosphatidylcholine; MAG: myelin-associated glycoprotein; PBS: phosphate buffered saline; RT-PCR: reverse-transcription polymerase chain reaction; TEM: transmission electron microscopy; WT: wild-type

Acknowledgements

We gratefully acknowledge R. Fujita, N. Kiguchi, and T. Suematsu for technical help with the TEM studies. This work was supported by MEXT KAKENHI (17109015 to Hiroshi Ueda; 21600008 to Mutsumi Ueda) and NIH grant (MH51699 and NS048478 to Jerold Chun). AstraZeneca Foundation, ONO Medical Research Foundation and Health Labor Sciences Research Grants from the Ministry of Health, Labor and Welfare of Japan (to Hiroshi Ueda): "Research on Allergic disease and Immunology" and "Third Term Comprehensive Control Research for Cancer (398-49)" also supported this work.

Author details

[1]Division of Molecular Pharmacology and Neuroscience, Nagasaki University Graduate School of Biomedical Sciences, 1-14 Bunkyo-machi, Nagasaki 852-8521, Japan. [2]Division of Pharmacology 1, Nagasaki University Graduate School of Biomedical Sciences, 1-12-4 Sakamoto, Nagasaki 852-8523, Japan. [3]Laboratory of Molecular and Cellular Biochemistry, Graduate School of Pharmaceutical Sciences, Tohoku University, 6-3 Aobayama, Aoba-ku, Sendai 980-8578, Japan. [4]Department of Molecular Biology, The Scripps Research Institute, La Jolla, CA 92037, USA.

Authors' contributions

JN contributed to the experiment on demyelination and the writing the manuscripts. H Uchida participated in the RT-PCR study and writing the manuscripts. YM performed experiments on demyelination. RY performed experiments on immunohistochemistry. MU and MN participated in the writing the manuscripts. JC generated $Lpar1^{-/-}$ mice. JA generated recombinant ATX and $atx^{+/-}$ mice. H Ueda is responsible for the experimental design and writing the manuscript. All authors read and approved the final manuscript.

Competing interests

The authors declare that they have no competing interests.

Received: 28 July 2010 Accepted: 9 November 2010
Published: 9 November 2010

References

1. Carter GT, Jensen MP, Galer BS, Kraft GH, Crabtree LD, Beardsley RM, Abresch RT, Bird TD: **Neuropathic pain in Charcot-Marie-Tooth disease.** *Arch Phys Med Rehabil* 1998, **79(12)**:1560-1564.
2. Svendsen KB, Jensen TS, Hansen HJ, Bach FW: **Sensory function and quality of life in patients with multiple sclerosis and pain.** *Pain* 2005, **114(3)**:473-481.
3. Gillespie CS, Sherman DL, Fleetwood-Walker SM, Cottrell DF, Tait S, Garry EM, Wallace VC, Ure J, Griffiths IR, Smith A, *et al*: **Peripheral demyelination and neuropathic pain behavior in periaxin-deficient mice.** *Neuron* 2000, **26(2)**:523-531.
4. Wallace VC, Cottrell DF, Brophy PJ, Fleetwood-Walker SM: **Focal lysolecithin-induced demyelination of peripheral afferents results in neuropathic pain behavior that is attenuated by cannabinoids.** *J Neurosci* 2003, **23(8)**:3221-3233.
5. Olechowski CJ, Truong JJ, Kerr BJ: **Neuropathic pain behaviours in a chronic-relapsing model of experimental autoimmune encephalomyelitis (EAE).** *Pain* 2009, **141(1-2)**:156-164.
6. Moalem-Taylor G, Allbutt HN, Iordanova MD, Tracey DJ: **Pain hypersensitivity in rats with experimental autoimmune neuritis, an animal model of human inflammatory demyelinating neuropathy.** *Brain Behav Immun* 2007, **21(5)**:699-710.
7. Ahn DK, Lee SY, Han SR, Ju JS, Yang GY, Lee MK, Youn DH, Bae YC: **Intratrigeminal ganglionic injection of LPA causes neuropathic pain-like behavior and demyelination in rats.** *Pain* 2009, **146(1-2)**:114-120.
8. Inoue M, Rashid MH, Fujita R, Contos JJ, Chun J, Ueda H: **Initiation of neuropathic pain requires lysophosphatidic acid receptor signaling.** *Nat Med* 2004, **10(7)**:712-718.
9. Fujita R, Kiguchi N, Ueda H: **LPA-mediated demyelination in ex vivo culture of dorsal root.** *Neurochemistry International* 2007, **50(2)**:351-355.
10. Ma L, Uchida H, Nagai J, Inoue M, Aoki J, Ueda H: **Evidence for De Novo Synthesis of Lysophosphatidic Acid in the Spinal Cord through Phospholipase A2 and Autotaxin in Nerve Injury-induced Neuropathic Pain.** *J Pharmacol Exp Ther* 2010, **333(2)**:540-546.
11. Inoue M, Ma L, Aoki J, Chun J, Ueda H: **Autotaxin, a synthetic enzyme of lysophosphatidic acid (LPA), mediates the induction of nerve-injured neuropathic pain.** *Mol Pain* 2008, **4**:6.
12. Contos JJ, Fukushima N, Weiner JA, Kaushal D, Chun J: **Requirement for the lpA1 lysophosphatidic acid receptor gene in normal suckling behavior.** *Proc Natl Acad Sci USA* 2000, **97(24)**:13384-13389.
13. Tanaka M, Okudaira S, Kishi Y, Ohkawa R, Iseki S, Ota M, Noji S, Yatomi Y, Aoki J, Arai H: **Autotaxin stabilizes blood vessels and is required for**

embryonic vasculature by producing lysophosphatidic acid. *J Biol Chem* 2006, **281(35)**:25822-25830.
14. Zimmermann M: **Ethical guidelines for investigations of experimental pain in conscious animals.** *Pain* 1983, **16(2)**:109-110.
15. Malmberg AB, Basbaum AI: **Partial sciatic nerve injury in the mouse as a model of neuropathic pain: behavioral and neuroanatomical correlates.** *Pain* 1998, **76(1-2)**:215-222.
16. Hylden JL, Wilcox GL: **Intrathecal morphine in mice: a new technique.** *Eur J Pharmacol* 1980, **67(2-3)**:313-316.
17. Hecht JH, Weiner JA, Post SR, Chun J: **Ventricular zone gene-1 (vzg-1) encodes a lysophosphatidic acid receptor expressed in neurogenic regions of the developing cerebral cortex.** *J Cell Biol* 1996, **135(4)**:1071-1083.
18. Marchand F, Perretti M, McMahon SB: **Role of the immune system in chronic pain.** *Nat Rev Neurosci* 2005, **6(7)**:521-532.
19. Garbay B, Heape AM, Sargueil F, Cassagne C: **Myelin synthesis in the peripheral nervous system.** *Prog Neurobiol* 2000, **61(3)**:267-304.
20. Quarles RH: **A hypothesis about the relationship of myelin-associated glycoprotein's function in myelinated axons to its capacity to inhibit neurite outgrowth.** *Neurochem Res* 2009, **34(1)**:79-86.
21. Georgiou J, Tropak MP, Roder JC: **Myelin-associated glycoprotein gene.** In *Myelin biology and disorders.* Edited by: Lazzarini RA. Elsevier Academic Press, San Diego; 2004:421-467.
22. Inoue M, Xie W, Matsushita Y, Chun J, Aoki J, Ueda H: **Lysophosphatidylcholine induces neuropathic pain through an action of autotaxin to generate lysophosphatidic acid.** *Neuroscience* 2008, **152(2)**:296-298.
23. Nave KA, Trapp BD: **Axon-glial signaling and the glial support of axon function.** *Annu Rev Neurosci* 2008, **31**:535-561.
24. Ueda H: **Peripheral mechanisms of neuropathic pain - involvement of lysophosphatidic acid receptor-mediated demyelination.** 2008, **4**:11.
25. Ueda H: **Molecular mechanisms of neuropathic pain-phenotypic switch and initiation mechanisms.** *Pharmacol Ther* 2006, **109(1-2)**:57-77.
26. Devor M: **Response of nerves to injury in relation to neuropathic pain.** In *Wall and Melzack's textbook of pain.* Edited by: McMahon SB, Koltzenburg M. Oxford: Churchill Livingstone; 2006:905-927.
27. Gupta R, Rummler LS, Palispis W, Truong L, Chao T, Rowshan K, Mozaffar T, Steward O: **Local down-regulation of myelin-associated glycoprotein permits axonal sprouting with chronic nerve compression injury.** *Exp Neurol* 2006, **200(2)**:418-429.
28. Woolf C, Salter M: **Plasticity and pain: role of the dorsal horn.** In *Wall and Melzack's textbook of pain.* Edited by: McMahon SB, Koltzenburg M. Oxford: Churchill Livingstone; 2006:91-105.
29. Inoue M, Ma L, Aoki J, Ueda H: **Simultaneous stimulation of spinal NK1 and NMDA receptors produces LPC which undergoes ATX-mediated conversion to LPA, an initiator of neuropathic pain.** *J Neurochem* 2008, **107(6)**:1556-1565.
30. Chattopadhyay S, Myers RR, Janes J, Shubayev V: **Cytokine regulation of MMP-9 in peripheral glia: implications for pathological processes and pain in injured nerve.** *Brain Behav Immun* 2007, **21(5)**:561-568.
31. Kobayashi H, Chattopadhyay S, Kato K, Dolkas J, Kikuchi S, Myers RR, Shubayev VI: **MMPs initiate Schwann cell-mediated MBP degradation and mechanical nociception after nerve damage.** *Mol Cell Neurosci* 2008, **39(4)**:619-627.
32. Xie W, Uchida H, Nagai J, Ueda M, Chun J, Ueda H: **Calpain-mediated down-regulation of myelin-associated glycoprotein in lysophosphatidic acid-induced neuropathic pain.** *J Neurochem* 2010, **113(4)**:1002-1011.
33. Bhangoo S, Ren D, Miller RJ, Henry KJ, Lineswala J, Hamdouchi C, Li B, Monahan PE, Chan DM, Ripsch MS, *et al*: **Delayed functional expression of neuronal chemokine receptors following focal nerve demyelination in the rat: a mechanism for the development of chronic sensitization of peripheral nociceptors.** *Mol Pain* 2007, **3**:38.
34. Woodruff RH, Franklin RJ: **Demyelination and remyelination of the caudal cerebellar peduncle of adult rats following stereotaxic injections of lysolecithin, ethidium bromide, and complement/anti-galactocerebroside: a comparative study.** *Glia* 1999, **25(3)**:216-228.
35. Ma L, Uchida H, Nagai J, Inoue M, Chun J, Aoki J, Ueda H: **Lysophosphatidic acid-3 receptor-mediated feed-forward production of lysophosphatidic acid: an initiator of nerve injury-induced neuropathic pain.** *Mol Pain* 2009, **5(1)**:64.

doi:10.1186/1744-8069-6-78
Cite this article as: Nagai *et al.*: Autotaxin and lysophosphatidic acid$_1$ receptor-mediated demyelination of dorsal root fibers by sciatic nerve injury and intrathecal lysophosphatidylcholine. *Molecular Pain* 2010 6:78.

Journal of Neurochemistry

JOURNAL OF NEUROCHEMISTRY | 2010 | 115 | 643–653 doi: 10.1111/j.1471-4159.2010.06955.x

Microglial activation mediates *de novo* lysophosphatidic acid production in a model of neuropathic pain

Lin Ma, Jun Nagai and Hiroshi Ueda

Division of Molecular Pharmacology and Neuroscience, Nagasaki University Graduate School of Biomedical Sciences, Bunkyo-machi, Nagasaki, Japan

Abstract

We recently demonstrated that *de novo* lysophosphatidic acid (LPA) production in the spinal cord occurs in the early phase after nerve injury or LPA injection, and underlies the peripheral mechanisms of neuropathic pain. In this study, we examined the possible involvement of spinal cord microglia in such LPA-mediated functions. Intrathecal LPA injection rapidly increased the gene expression of CD11b and protein expression of phosphor-p38, accompanied by a morphological change of microglia from a ramified to amoeboid shape. Although early treatment with minocycline significantly inhibited LPA-induced neuropathic pain-like behavior and microglial activation, late treatment did not. Early treatment with minocycline also blocked LPA-evoked *de novo* LPA production and the increased activation of cytosolic phospholipase A_2, an LPA synthesis-related enzyme. Similar results were observed when the sciatic nerve was partially injured: early, but not late, treatment with minocycline significantly inhibited the injury-induced neuropathic pain, microglial activation, *de novo* LPA production and the underlying increased activation of cytosolic phospholipase A_2 as well as calcium-independent phospholipase A_2, another LPA synthesis-related enzyme. These findings suggest that the early phase of microglial activation is involved in *de novo* LPA production, and that this underlies the initial mechanisms of nerve injury-induced neuropathic pain.

Keywords: lysophosphatidic acid, microglia, minocycline, nerve injury, neuropathic pain, p38.

J. Neurochem. (2010) **115**, 643–653.

We previously reported that lysophosphatidic acid-1 (LPA_1) receptor signaling initiates nerve injury-induced neuropathic pain and its underlying machineries, including up-regulation of the expression of the voltage-gated calcium channel $\alpha_2\delta$-1 subunit in the dorsal root ganglion, protein kinase Cγ in the spinal dorsal horn (SC) and demyelination of dorsal root (DR) fibers (Inoue *et al.* 2004; Ueda 2006, 2008). Further, a single intrathecal (i.t.) injection of LPA mimicked nerve injury-induced behavioral and biochemical changes (Inoue *et al.* 2004). The original concept that the neuropathic pain is initiated by LPA_1 signaling was confirmed by a pharmacological study using the short-lived LPA_1 antagonist Ki-16425, which only inhibited neuropathic pain behavior when given within a timeframe of 2–4 h after nerve injury (Ma *et al.* 2009a). Recently, we demonstrated that *de novo* LPA production plays a crucial role in the development of neuropathic pain caused by nerve injury or i.t. injection of LPA (Ma *et al.* 2009b, 2010). It should be noted that the timeframe of autotaxin (ATX)-mediated *de novo* LPA production was maximal at 2–3 h after the treatments and declined thereafter. Thus, *de novo* LPA production in the spinal cord and LPA_1 signaling in peripheral nerves may underlie the initial mechanisms of neuropathic pain.

For decades, neuropathic pain and its underlying mechanisms have been considered primarily in terms of plasticity in primary afferent neurons, such as altered gene expression and neuronal reorganization at the level of the SC (Ji *et al.* 1999;

Received May 18, 2010; revised manuscript received August 9, 2010; accepted August 10, 2010.

Address correspondence and reprint requests to Dr. Hiroshi Ueda, Division of Molecular Pharmacology and Neuroscience, Nagasaki University Graduate School of Biomedical Sciences, 1-14 Bunkyo-machi, Nagasaki 852-8521, Japan. E-mail: ueda@nagasaki-u.ac.jp

Abbreviations used: ATX, autotaxin; BSA, bovine serum albumin; $cPLA_2$, cytosolic phospholipase A_2; DMEM, Dulbecco's modified Eagle's medium; DR, dorsal root; HRP, horseradish peroxidase; i.p., intraperitoneal; i.t., intrathecal; Iba1, ionized calcium-binding adaptor molecule 1; $iPLA_2$, calcium-independent phospholipase A_2; LPA, lysophosphatidic acid; LPC, lysophosphatidylcholine; PBS, phosphate buffered saline; PC, phosphatidylcholine; p-p38, phosphor-p38; SC, spinal dorsal horn.

